

A new Early Triassic brachiopod fauna from southern Tibet, China: Implications on brachiopod recovery and the late Smithian extinction in southern Tethys

Fengyu Wang,¹ Jing Chen,^{2*} Xu Dai,¹ and Haijun Song¹

¹State Key Laboratory of Biogeology and Environmental Geology, School of Earth Sciences, China University of Geosciences, Wuhan, 430074, China <fengyuwang@cug.edu.cn>, <xudai@cug.edu.cn>, <haijunsong@cug.edu.cn>

²Yifu Museum, China University of Geosciences, Wuhan, 430074, China <jingchen@cug.edu.cn>

Abstract.—Brachiopods suffered high levels of extinction during the Permian–Triassic crisis, and their diversity failed to return to Permian levels. In the aftermath of the Permian–Triassic mass extinction, brachiopods were extremely rare worldwide, especially in the southern hemisphere. Here, we report a new Early Triassic brachiopod fauna from the Selong section in southern Tibet, China. A new genus and three new species have been identified: *Selongthyris plana* Wang and Chen n. gen. n. sp., *Piarorhynchella selongensis* Wang and Chen n. sp., and *Schwagerispira cheni* Wang and Chen n. sp., which are typical. The ontogenies and internal structures of these three new species are described in detail. This brachiopod fauna corresponds to the *Neospathodus pakistanensis* and *Neospathodus waageni* conodont biozones and *Kashmirites* and *Anasibirites* ammonoid biozones, indicating a late Dienerian to late Smithian age. The post-extinction recovery of brachiopods in the Himalayas may have begun by the early Smithian of the Early Triassic. In addition, these species did not persist into the Spathian substage, suggesting that the newly evolved brachiopods in the southern Tethys were severely affected by the late Smithian extinction event.

UUID: <http://zoobank.org/f8fc8ced-432c-41d2-8c6c-d17bca527109>

Introduction

The Permian–Triassic mass extinction was the most severe extinction event in Earth’s history, causing more than 90% of marine organisms to become extinct (Erwin, 1994; Song et al., 2013). Brachiopoda were among the most abundant benthos in the Paleozoic ocean, but they were no longer the dominant group of benthos after the Permian–Triassic crisis (Sun and Shen, 2004; Chen et al., 2005b; Shen et al., 2006a; Chen et al., 2015; Carlson, 2016; Ke et al., 2016). The Early Triassic brachiopods, except the surviving Permian-type brachiopods from the Permian–Triassic boundary and early Griesbachian (Chen et al., 2005a, b; Ke et al., 2016), are rare worldwide (Dagys, 1974, 1993; Ager, 1988; Ager and Sun, 1988; Chen et al., 2005b; Ke et al., 2016), with only 18 species (including seven undefined species) recorded in Griesbachian strata (Bittner, 1899a, b; Newell and Kummel, 1942; Dagys, 1965, 1974; Shen and He, 1994; Chen et al., 2002; F.Y. Wang et al., 2017; Dai et al., 2018), four species (including one undefined species) recorded in Dienerian strata (Dagys, 1965; Hoover, 1979; Shigeta et al., 2009; Hofmann et al., 2013; Zakharov and Popov, 2014), and 36 species (including seven undefined species) recorded in Olenekian strata (Girty, 1927; Dagys, 1974; Feng and Jiang, 1978; Hoover, 1979; Perry and Chatterton, 1979; Sun et al., 1981; Chen, 1983; Xu and Liu, 1983; Iordan,

1993; Shigeta et al., 2009; Hofmann et al., 2013, 2014; Zakharov and Popov, 2014; Popov and Zakharov, 2017; Sun et al., 2017; Grădinaru and Gaetani, 2019). However, 26 species (including seven undefined species) of Early Triassic brachiopods have been reported in Spathian strata (Hoover, 1979; Perry and Chatterton, 1979; Shigeta et al., 2009; Hofmann et al., 2013, 2014; Zakharov and Popov, 2014; Popov and Zakharov, 2017; Sun et al., 2017; Grădinaru and Gaetani, 2019).

The paleogeographical distribution of Early Triassic brachiopods is heterogenous between the two hemispheres. Brachiopods were more widely distributed in the northern hemisphere than in the southern hemisphere, and a total of 45 species (including 18 indeterminate species) were distributed from the low latitude to high latitude regions in the northern hemisphere throughout the Griesbachian to Spathian. These species include six from South China (Feng and Jiang, 1978; Shen and He, 1994; Chen et al., 2002; F.Y. Wang et al., 2017), 10 species from the western USA (Girty, 1927; Newell and Kummel, 1942; Hoover, 1979; Perry and Chatterton, 1979; Hofmann et al., 2013, 2014), five species from Romania (Iordan, 1993; Grădinaru and Gaetani, 2019), three species from the southern Qilian Mountains of China (Xu and Liu, 1983), seven species from Kazakhstan (Dagys, 1974; Zakharov and Popov, 2014), one species from northwest Caucasus (Dagys, 1974), and 20 species from South Primorye of Russia (Bittner, 1899b; Dagys, 1965, 1974; Shigeta et al., 2009; Zakharov and Popov, 2014; Popov and Zakharov, 2017). However, only six species have been reported in the southern hemisphere, including

*Corresponding author

three species from Lhasa in China (Sun et al., 1981), one species from Spiti in India (Bittner, 1899a), and two species from southern Tibet in China (Chen, 1983). Notably, the internal structures of most of these brachiopods from the southern hemisphere have not been well studied. Investigations regarding Early Triassic brachiopods in the southern hemisphere may give us a better understanding of the evolution, ecology, and paleobiogeography of the Early Triassic.

In this study, we report a new Early Triassic (late Dienerian–late Smithian) brachiopod fauna from the middle-upper part of the Kangshare Formation at the Selong section in southern Tibet. One new genus and three new species were systematically described. In addition, we studied the internal structures and ontogeny of these species in detail. Our findings may fill a gap in our knowledge of brachiopod biogeography.

Geological setting

The Selong section (84°49'E, 28°39'N) is located in Selong Village, Nyalam County, in southern Tibet, China (Fig. 1.1–1.3), and was previously proposed as a candidate of the Global Stratotype Section and Point of the Permian-Triassic boundary (Wang et al., 1989; Jin et al., 1996; Yuan et al., 2018). A detailed biostratigraphic framework was constructed at Selong using conodonts and ammonoids (Wang and He, 1976; Yao and Li, 1987; Wang et al., 1989; Orchard et al., 1994; Wang and Wang, 1995; Jin et al., 1996; Shen et al., 2006b; L.N. Wang et al., 2017; Yuan et al., 2018). In addition, sedimentology (Jin et al., 1996; Garzanti et al., 1998; Yuan et al., 2018; Li et al., 2019), geochemistry (Li et al., 2018; Yuan et al., 2018), and Permian-Triassic mass extinction patterns have also been studied (Shen et al., 2006b; Yuan et al., 2018).

The Selong section exposes a complete stratigraphic sequence from the uppermost Permian to the basal upper Lower Triassic strata (Fig. 2). There may be an unconformity between the Selong Group below the Permian-Triassic boundary and the Kangshare Formation above the boundary (Yuan et al., 2018). The lower part of the Selong Group consists of 24 m thick bioclastic limestone and dark silty shales, and the upper part consists of massive crinoid grainstone beds that contain abundant brachiopods, crinoids, bryozoans, and corals (Shen et al., 2000, 2001, 2006b; Sakagami et al., 2006; Yuan et al., 2018). The lowermost part of the Kangshare Formation is characterized by brown dolomitized crinoidal packstone and thick-bedded packstone beds (i.e., *Waagenites* Bed and *Otoceras* Bed), yielding brachiopods, corals, bryozoans, ammonoids, ostracodes, foraminifers, and calcareous sponges. The Permian-Triassic boundary is indicated by the first occurrence of the conodont *Hindeodus parvus* (Kozur and Pjatakova, 1976) at the bottom of the *Otoceras* Bed (Shen et al., 2000, 2006b; Yuan et al., 2018). The overlying strata consist of khaki thin- to medium-bedded packstone/wackestone beds, which are dominated by abundant ammonoids, brachiopods, and bivalves. The middle portion of the Kangshare Formation is a set of black shales, in which there are two packstone/wackestone layers. The overlying strata are dominated by reddish to yellowish and ferruginous wackestone layers consisting of abundant brachiopods and a small number of ammonoids. This part

includes gray and thin- to medium-bedded packstone/wackestone carbonates that are rich in ammonoids, bivalves, and brachiopods. Farther up, another set of black shales crops out. Above the shale strata are 2 m thick packstone/wackestone beds, which constitute the uppermost part of the Lower Triassic.

A high-resolution biostratigraphic framework was established based on the conodont and ammonoid records from the Selong section (Yao and Li, 1987; Wang et al., 1989; Orchard et al., 1994; Wang and Wang, 1995; An et al., 2018). Occurrences of the conodont *Neospathodus pakistanensis* Sweet, 1970 (Wang et al., 1989; Wang and Wang, 1995; An et al., 2018) and ammonoid *Koninckites vetustus* Waagen, 1895 (Figs. 2, 3) in Beds 29–33 indicate a late Dienerian age. The conodont *Neospathodus waageni* Sweet, 1970, and ammonoid *Kashmirites* occur in Beds 35–42, suggesting an early Smithian age (Brühwiler et al., 2010) (Figs. 2, 3). The overlying brachiopods in Beds 67–70 co-occurred with the ammonoid *Anasibirites*, indicating their occurrence during the late Smithian age (Wang and He, 1976; Wang et al., 1989). Based on the conodont and ammonoid data mentioned above, the abundant brachiopods in Beds 29, 35–42, and 67–70 (Fig. 2) occurred during the late Dienerian–late Smithian age.

Materials and methods

There were 825 brachiopod specimens collected from the Kangshare Formation in the Selong section. The external features, internal structure, and ontogeny of these specimens have been systematically studied. The Selong fauna contains three brachiopod species from three genera: *Piarorhynchella selongensis* Wang and Chen n. sp. (612 specimens), *Schwagerispira cheni* Wang and Chen n. sp. (181 specimens), and *Selongthyris plana* Wang and Chen n. gen. n. sp. (32 specimens). Despite these brachiopods being extremely small, most of them were completely preserved. However, the Early Triassic brachiopods and some Middle Triassic brachiopods were difficult to identify because of their similarities in both their internal and external features. In order to accurately identify the Selong brachiopods, the external and internal characteristics were studied in detail, and the ontogenetic characteristics of each species were fully considered. Moreover, a comprehensive review of related species was carried out, focusing on the characteristics of intraspecific variation and individual development. The external features of juveniles to adults of each species in a large number of specimens were carefully studied. All specimens were photographed using a Canon 6D Mark II camera with a macro lens EF 100 mm f/2.8. To accurately assess the characteristics of the internal structures, 17 specimens (10 specimens of *Piarorhynchella selongensis* n. sp., four specimens of *Schwagerispira cheni* n. sp., and three specimens of *Selongthyris plana* n. gen. n. sp.) were selected to grind serial sections. The minimal distance among serial sections is 0.01 mm. There were 414 serial sections produced, each of which was observed and photographed under a Leica S8 APO stereo microscope.

Repository and institutional abbreviation.—All described specimens in this study are deposited in the Yifu Museum of China University of Geosciences, Wuhan, China (collection number CUG SL-A-001-SL-C-825).

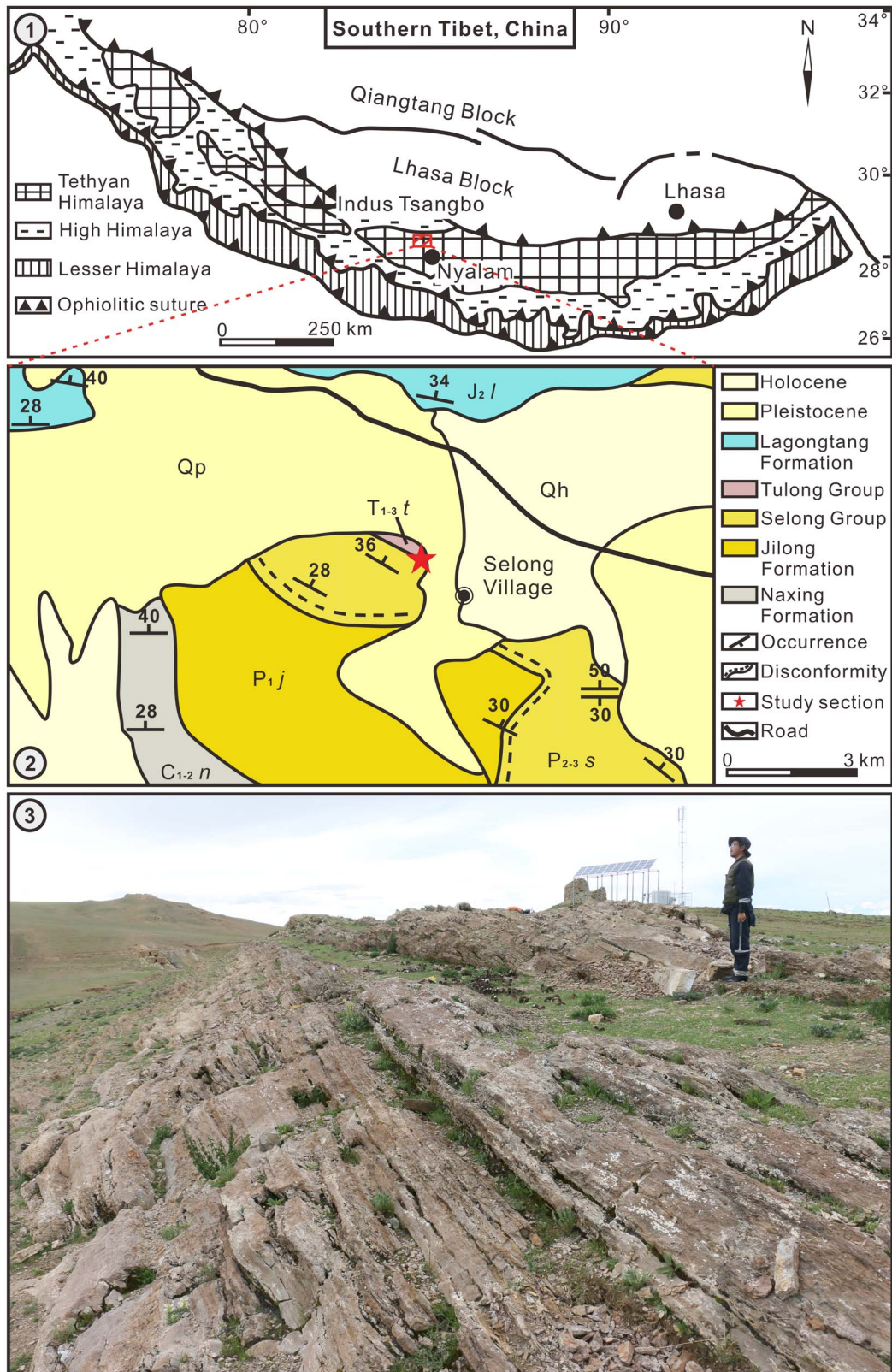


Figure 1. (1) Geological map of southern Tibet, China, modified from Li et al. (2019). (2) Geological map of Selong area, showing the studied section. (3) Field view of Selong section. C_{1-2 n} = Lower and middle Carboniferous Naxing Formation; P_{1 j} = lower Permian Jilong Formation; P_{2-3 s} = middle and upper Permian Selong Group; T_{1-3 t} = Lower and Upper Triassic Tulong Group; J_{2 l} = Middle Jurassic Lagongtang Formation; Qp, Pleistocene; Qh, Holocene.

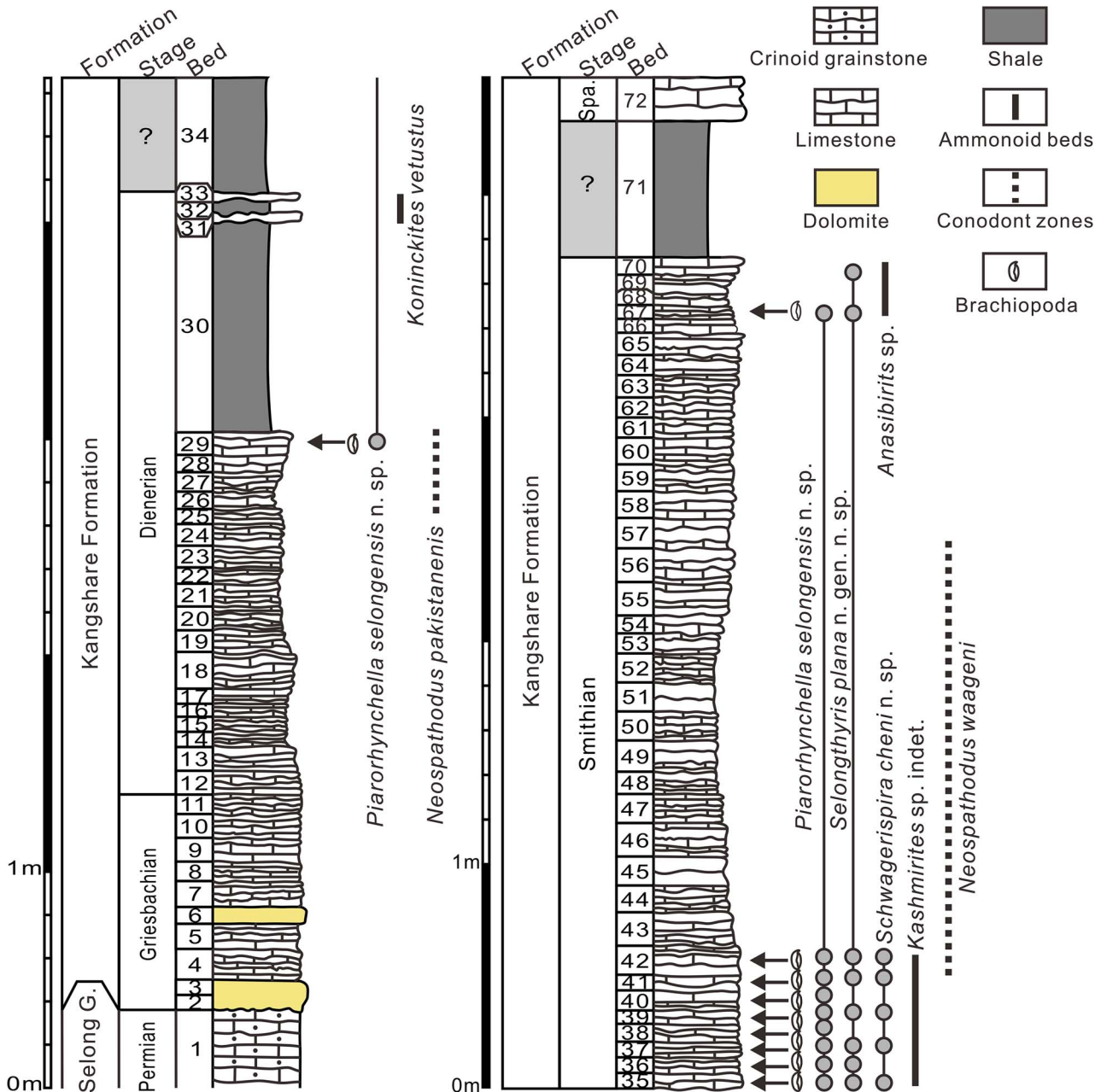


Figure 2. Lithology of the Selong Group and the Kangshare Formation at Selong section, showing the distribution of brachiopods. Conodont biozones and part of ammonoid beds modified from Wang et al. (1989) and An et al. (2018). Spa. = Spathian.

Systematic paleontology

The classification of the Brachiopoda adopted herein follows the revised Treatise on Invertebrate Paleontology, Part H (Williams et al., 2002, 2006).

- Order Rhynchonellida Kuhn, 1949
- Superfamily Norelloidea Ager, 1959
- Family Norellidae Ager, 1959
- Subfamily Holcorhynchellinae Dagys, 1974
- Genus *Piarorhynchella* Dagys, 1974

Type species.—*Piarorhynchella mangyshlakensis* Dagys, 1974; Karatauchik Range, Dolnapa Well, Mangyshlak; Olenekian.

Piarorhynchella selongensis Wang and Chen new species
 Figures 4–12

1983 *Nudirostralina subtrinodosi*; Chen, p. 155, pl. 1, fig. 2.

Syntypes.—Specimens SL-A-035 (Fig. 5.46–5.50) and SL-A-053 (Fig. 6.51–6.55), from the Early Triassic Kangshare Formation in the Selong section in southern Tibet, China.

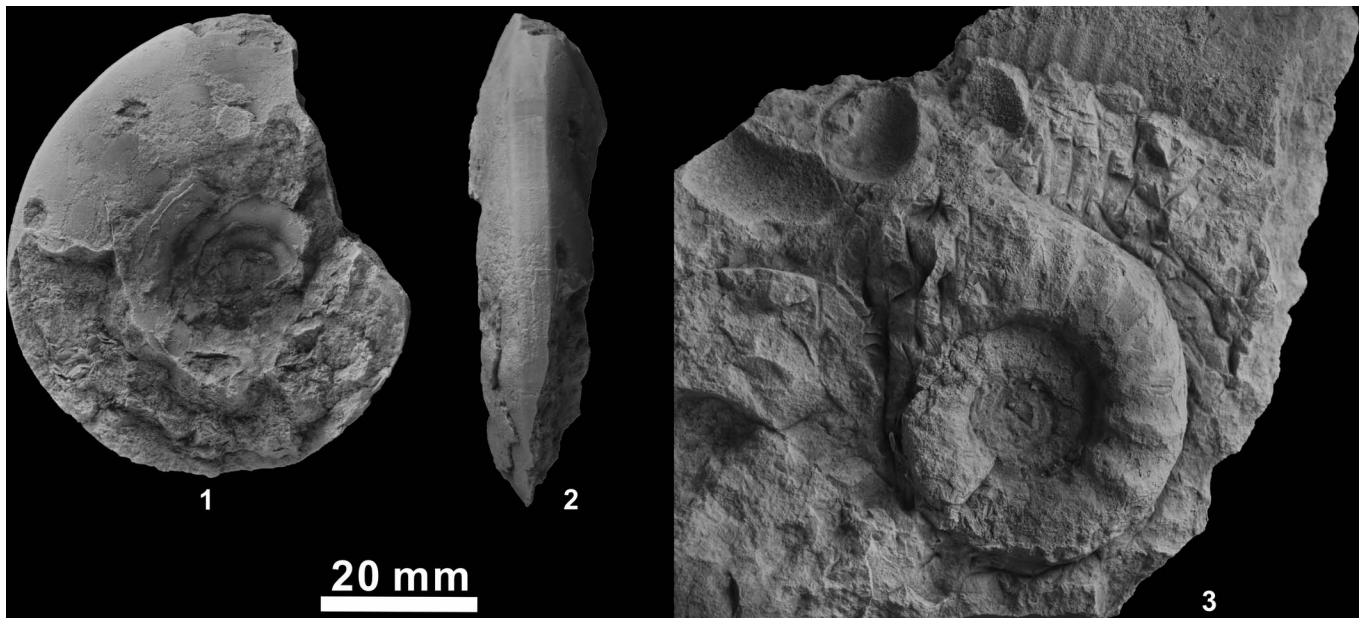


Figure 3. Ammonoids from the Kangshare Formation from Selong section, southern Tibet. (1, 2) *Koninckites vetustus* Waagen, 1895 (SL-AMM-001); (3) *Kashmirites* sp. indet. (SL-AMM-002).

Paratypes.—Specimens SL-A-033 (Fig. 5.36–5.40), SL-A-034 (Fig. 5.41–5.45), and SL-A-052 (Fig. 6.36–6.40), from the Early Triassic Kangshare Formation in the Selong section in southern Tibet, China.

Diagnosis.—Small-sized biconvex and subpentagonal shells; width slightly larger than the length, maximum width located in the anterior third. Fold and sulcus moderately developed. Posterior smooth, short plicae near anterior. Plicae range from 2–3 plicae in the dorsal fold, 1–2 in the ventral sulcus, and 1–2 poorly developed plicae on lateral flanks. Ventral valve with strong hinge teeth. Median septum absent. Dorsal valve with well-developed and steady median septum up to half length of shell in size. Septalium distinct but shallow. Crural bases distinct, subtriangular in shape. Crura raduliform.

Occurrence.—Kangshare Formation of late Dienerian–late Smithian age, Selong section, southern Tibet, China.

Description.—Subpentagonal in outline. Small size, 1.88–10.06 mm long, 1.73–11.21 mm wide; width slightly larger than the length (Fig. 8.1); maximum width reaches three-thirds of length anteriorly. Bioconvex in profile, the convexity of the dorsal valve slightly greater than that of the ventral valve, but shell flat; 0.55–6.32 mm thick, maximum thickness lies in the mid-length. Postero-lateral margin straight; anterior margin straight. Hinge line short and curved, much shorter than the maximal width. Fold and sulcus only appear anteriorly. Anterior commissure uniplicate to bisulcate. Trapezoidal linguiform extension short and slightly curved; beveled at low or medium angle to the plane of commissure. Shell smooth posteriorly, short and weak plicae near anterior margin.

Ventral valve mildly convex and most convex approximately in the middle of the shell. Umbo mildly convex, middle

part flat, anterior part extends forward and slightly bent. Apical angles 75–113°. Beak very distinct, small, pointed, slightly curved. Beak ridges round and curved, slightly convex to the plane of symmetry. Interarea short and narrow, but distinct. Foramen tiny, hypothyrid, oval or rounded triangular in shape. Deltidial plates disjunct. Sulcus develops from the middle of the shell, extremely shallow and flat posteriorly, and gradually widens towards anterior and starts to appear at one-fourth to one-sixth of the length anteriorly. Bottom of the sulcus flat and very shallow. Sulcus extends forward and slightly curved, forming trapezoidal linguiform extension, and never perpendicular to the commissure plane, forming geniculate commissure. Width of base accounts for 0–85% of the maximum width (Fig. 9.2). Width of top edge accounts for 0–68% of the maximum width (Fig. 9.1). Height of trapezoidal linguiform accounts for 0–95% of the maximum thickness (Fig. 9.3, 9.4). One to two plicae on the sulcus.

Dorsal valve mildly convex, most convex approximately in the middle of the shell. Umbo strongly curved, middle and anterior part slightly bent forward at the same degree. Beak strongly incurved and embedded into the ventral valve. Median sulcus very weak and shallow; appears from umbonal region where it is extremely weak, then extends forward and is replaced by the fold when there are three plicae on the fold, or continuously extends to the anterior region, forming shallow interspace between the two plicae when there are two plicae on the fold. Dorsal median fold moderately developed, begins in the mid-length, and becomes obvious on one-third to one-fourth of anterior area where one or three plicae present.

Shells covered by dense concentric growth lines. Short plicae only developed in the anterior region, about one-third to one-fourth of anterior area. Plicae blunt, rounded triangular in cross section. One to two identical plicae on the sulcus and

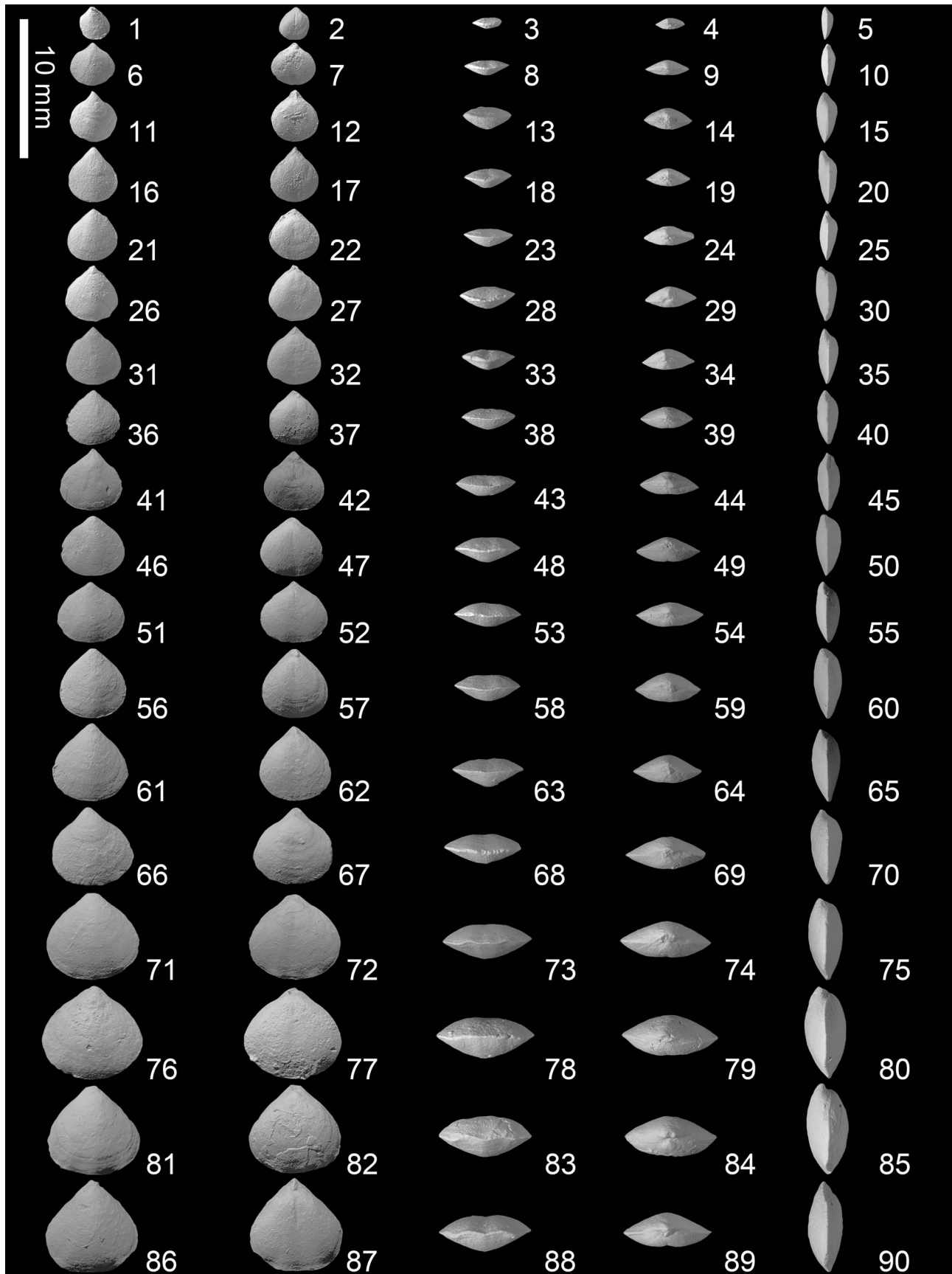


Figure 4. *Piarorhynchella selongensis* Wang and Chen n. sp. from the Kangshare Formation of Selong section, southern Tibet. For each articulated shell we present ventral, dorsal, anterior, posterior, and lateral views. (1–5) SL-A-001; (6–10) SL-A-002; (11–15); (16–20) SL-A-004; (21–25) SL-A-005; (26–30) SL-A-006; (31–35) SL-A-007; (36–40) SL-A-008; (41–45) SL-A-009; (46–50) SL-A-010; (51–55) SL-A-011; (56–60) SL-A-012; (61–65) SL-A-013; (66–70) SL-A-014; (71–75) SL-A-015; (76–80) SL-A-016; (81–85) SL-A-017; (86–90) SL-A-018.

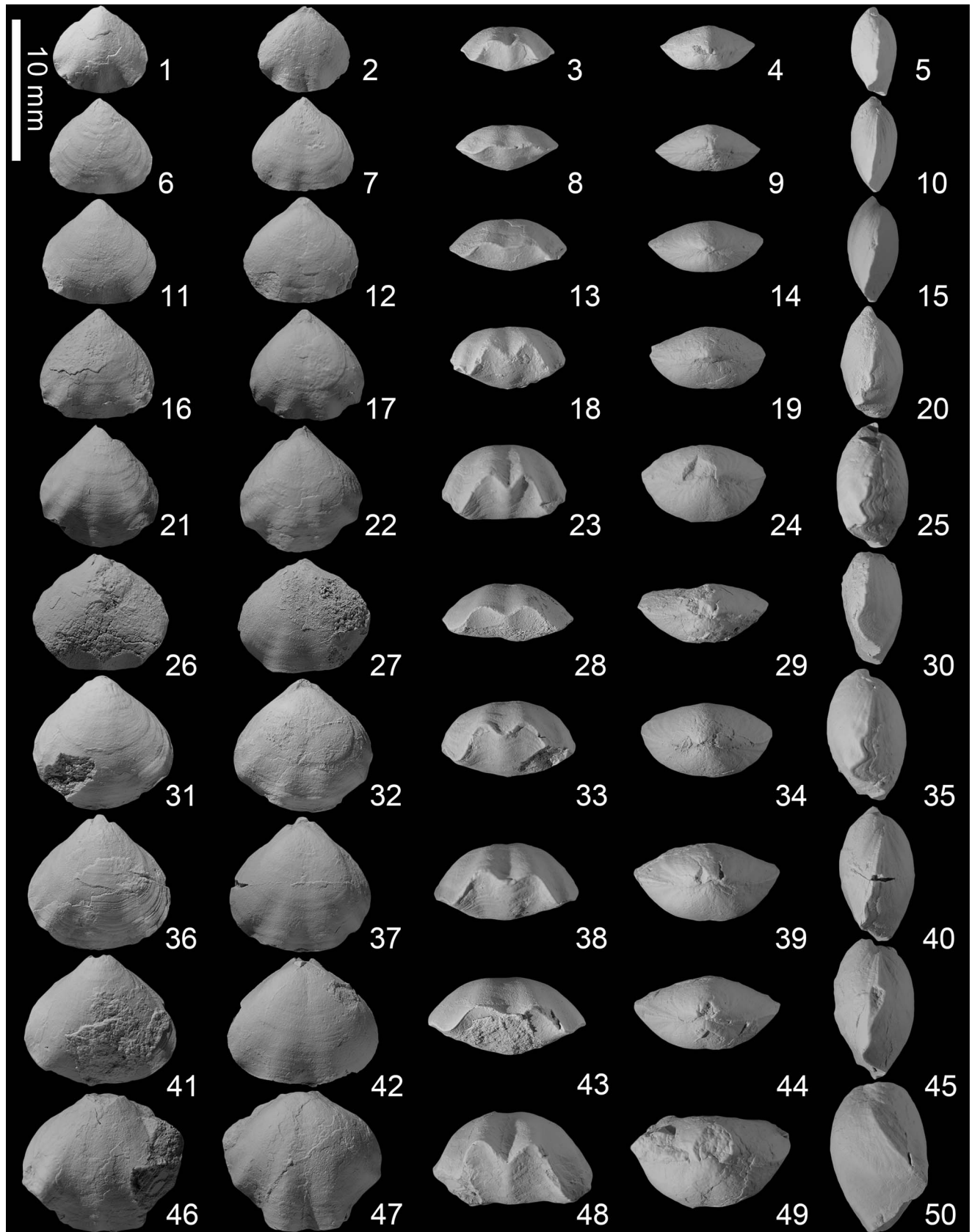


Figure 5. *Piarorhynchella selongensis* Wang and Chen n. sp. from the Kangshare Formation of Selong section, southern Tibet. For each articulated shell we present ventral, dorsal, anterior, posterior, and lateral views. (1–5) SL-A-019; (6–10) SL-A-023; (11–15) SL-A-026; (16–20) SL-A-027; (21–25) SL-A-030; (26–30) SL-A-029; (31–35) SL-A-032; (36–40) paratype SL-A-033; (41–45) paratype SL-A-034; (46–50) syntype SL-A-035.

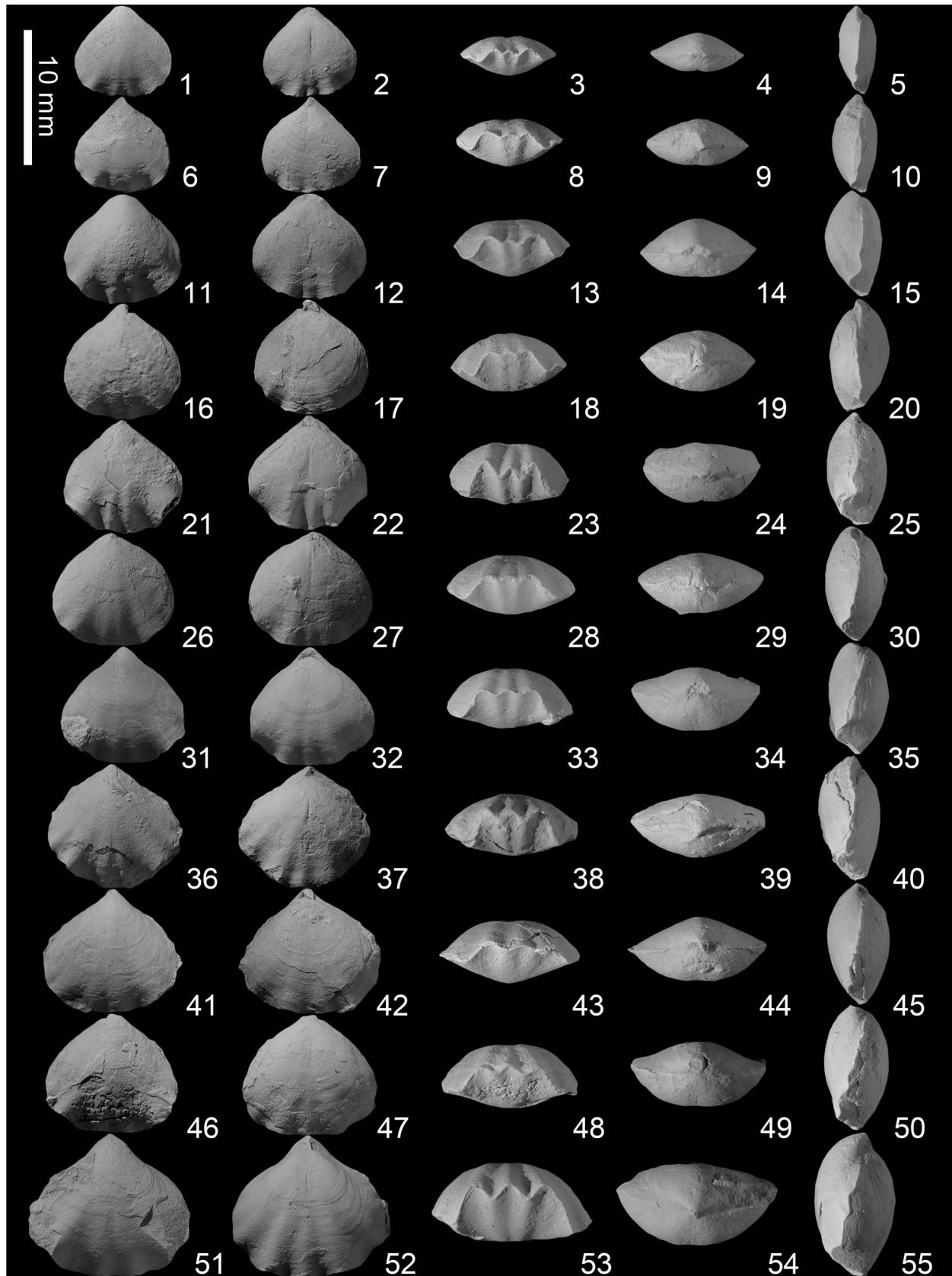


Figure 6. *Piarorhynchella selongensis* Wang and Chen n. sp. from the Kangshare Formation of Selong section, southern Tibet. For each shell we present ventral, dorsal, anterior, posterior, lateral views from the right to left side. (1–5) SL-A-036; (6–10) SL-A-039; (11–15) SL-A-041; (16–20) SL-A-043; (21–25) SL-A-044; (26–30) SL-A-046; (31–35) SL-A-047; (36–40) paratype SL-A-052; (41–45) SL-A-050; (46–50) SL-A-051; (51–55) syntype SL-A-053.

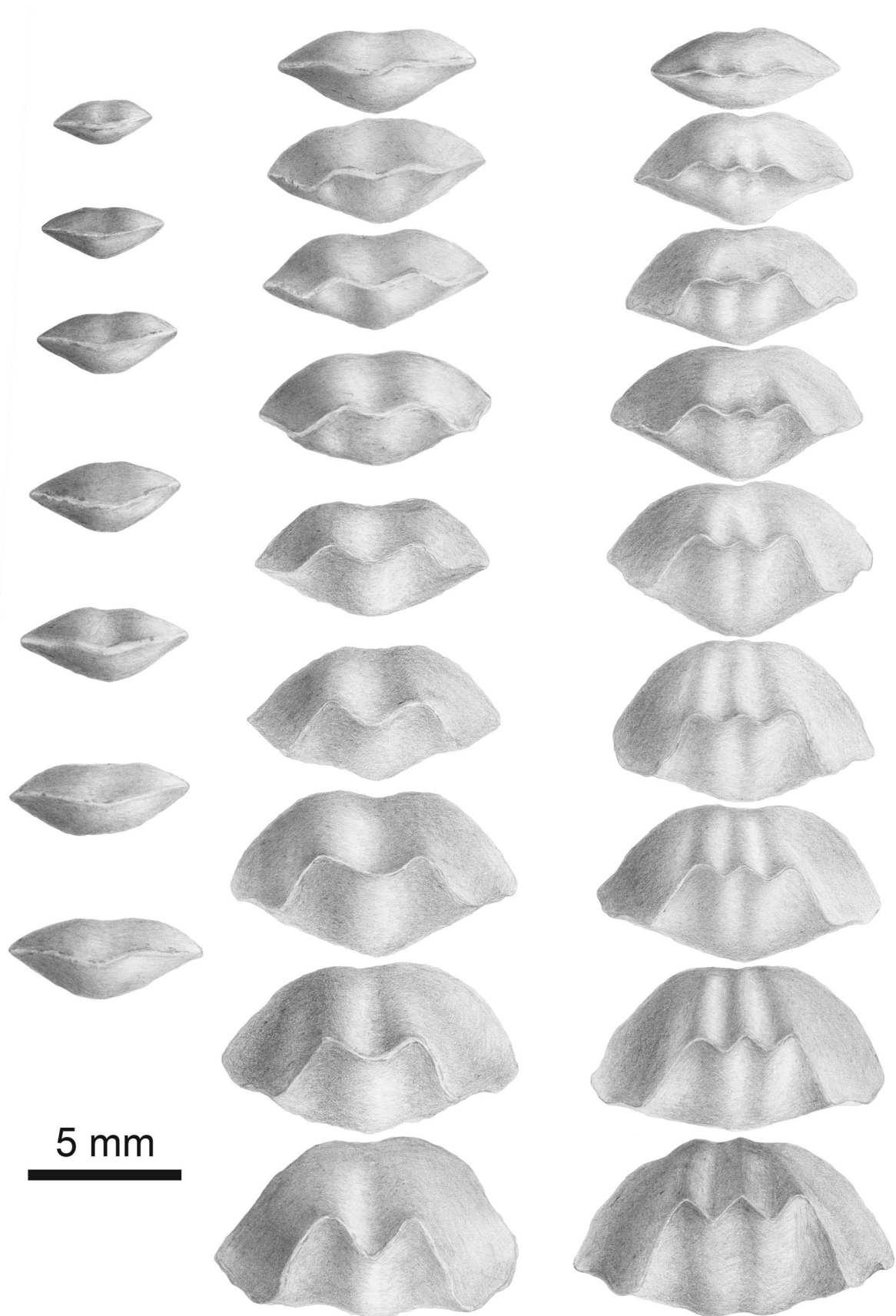


Figure 7. Ontogenesis of *Piarorhynchella selongensis* Wang and Chen n. sp. showing two different growth patterns.

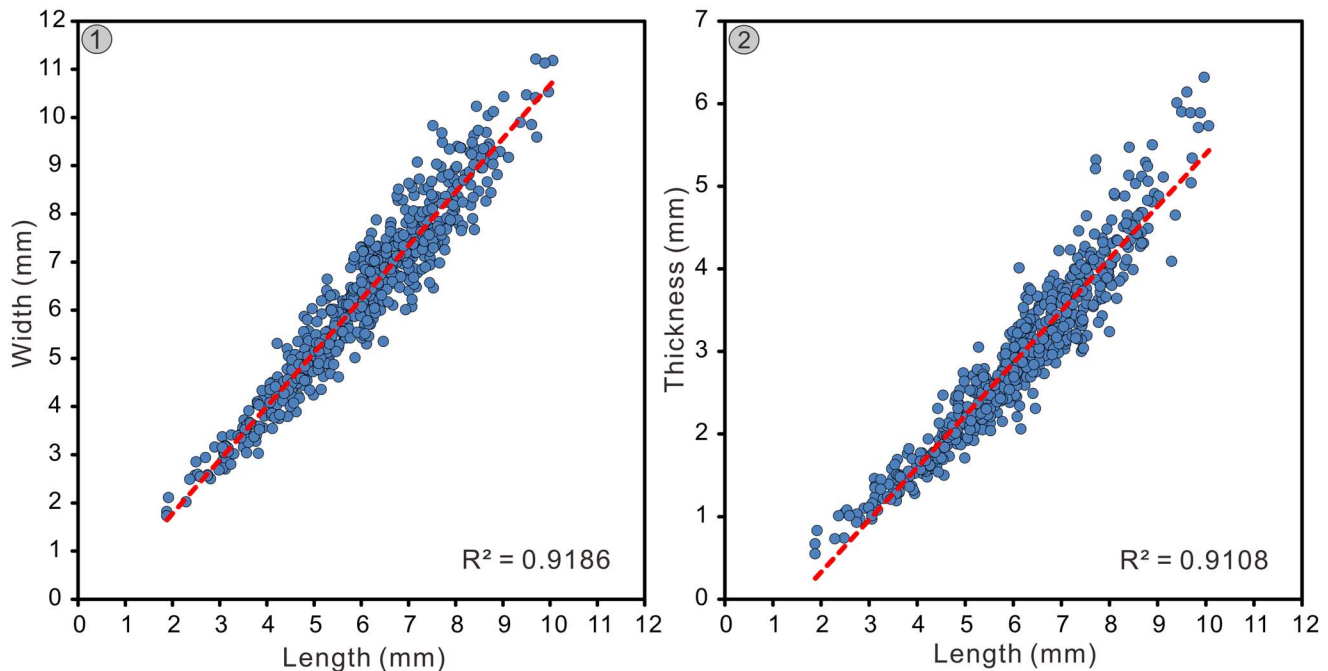


Figure 8. (1) Scatter plot of length/width of 612 articulated shells of *Piarorhynchella selongensis* Wang and Chen n. sp. (2) Scatter plot of length/thickness of the same. The red dotted line represents the trend line.

linguiform extension. Fold bears two to three identical plicae. Two arrangements of plicae in matured specimens, either three plicae on fold with two in sulcus (3/2, 50%) or two plicae on fold and one on sulcus (2/1, 50%). Plicae in the lateral flanks generally undeveloped, especially those closer to the posterolateral margin. One to two plicae only develop on lateral flanks. First lateral plicae appear at one-third of the length anteriorly, located at the two sides of the fold and sulcus of both valves. Second lateral plicae much wider, weaker, and shorter than any other, and appear only at the outermost lateral margin occasionally. Small bends next to the two lateral plicae only appear at the lateral commissure and never form real plicae on the shell surface in a few of the largest specimens.

Ventral delthyrial cavity oval to round. Pedicle collar absent. Dental plates thin and distinct, always straight, but the dip orientation varies. Dental plates nearly parallel, to ventrally convergent. Hinge teeth very strong with a large base and bifid; denticula absent or not developed. Sockets in dorsal valve well developed, mildly deep, with wide and flat bottom. Inner socket ridges and the outer socket ridges bend slightly toward each other; inner socket ridges incline toward medial. Hinge plates thin but very distinct, narrow posteriorly, wide anteriorly. Outer hinge plates nearly straight. Inner hinge plates slightly incline to the middle, connect to the median septum, forming distinct U- or V-shaped septalium, and become wider and deeper anteriorly. Median septum extends to half of length or more of the dorsal valve. Crural bases very distinct and triangular. Crura short, raduliform, nearly straight in the posterior area, symmetrically extend anteroventrally, and hook-like. Crura subtriangular, becoming increasingly thinner towards anterior and eventually becoming curved, subvertical plates in serial sections.

Etymology.—After the Selong section, from which the specimens were collected.

Material.—A total of 612 complete specimens collected from the Early Triassic Kangshare Formation. Of these, 10 specimens were sectioned (SL-A-SS-001, SL-A-SS-002 [Figs. 10, 11], SL-A-SS-003, SL-A-SS-004, SL-A-SS-005, SL-A-SS-006, SL-A-SS-007, SL-A-SS-008, SL-A-SS-009, SL-A-SS-010) and 39 selected specimens were photographed.

Remarks.—Some rhynchonellid species, attributed to nine genera (*Piarorhynchella* Dagys, 1974; *Abrekia* Dagys, 1974; *Nudirostralina* Yang and Xu, 1966; *Paranorellina* Dagys, 1974; *Laevorhynchia* Shen and He, 1994; *Meishanorhynchia* Chen and Shi in Chen et al., 2002; *Lichuanorelloides* F.Y. Wang et al., 2017; *Lissorhynchia* Yang and Xu, 1966; *Preliissorhynchia* Xu and Grant, 1994), share many external (especially in juvenile stages) and internal features and show relatively large intraspecific variation. Therefore, it is necessary to pay more attention to ontogeny and intraspecific variation in order to identify Triassic brachiopod species accurately, rather than just focusing on characteristic external features. As for internal structures, crura should be regarded as among the most important and valuable characteristics for classification because their features are relatively complex and generally consistent (Ager, 1965; Ager et al., 1972; Shi and Grant, 1993; Manceñido and Owen, 1996, 2001; Savage et al., 2002; Manceñido and Motchurova-Dekova, 2010).

Considering that the specimens, which were collected in contemporary strata from adjacent Tulong section (Chen, 1983) and Selong section (this study) in southern Tibet, China, have similar external features, we judge that they should belong to the same species. However, Chen (1983) identified

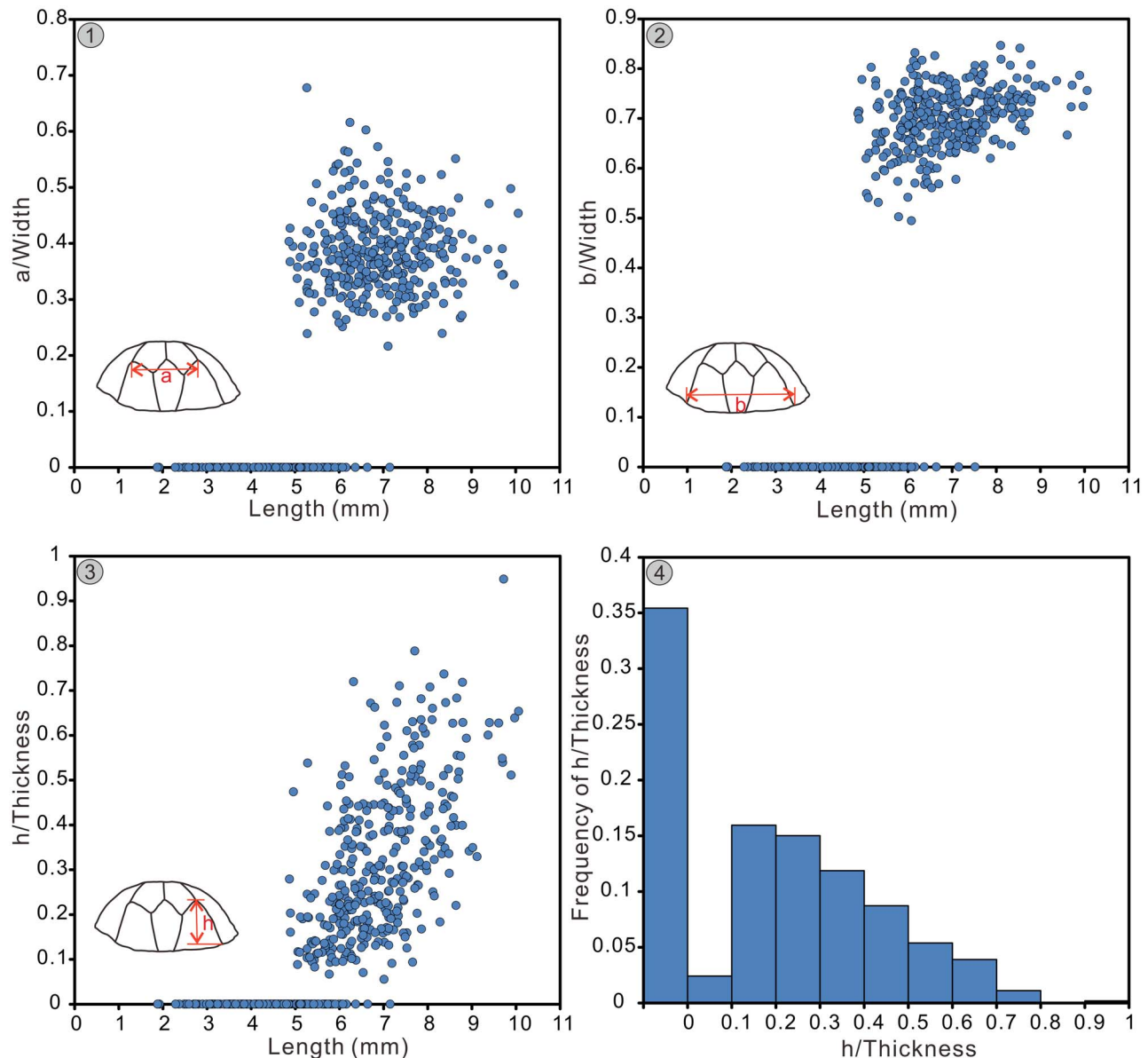


Figure 9. (1) Scatter plot of length/a/width of 612 articulated shells of *Piarorhynchella selongensis* Wang and Chen n. sp. (2) Scatter plot of length/b/width of the same. (3) Scatter plot of length/h/thickness of the same. (4) Frequency histogram of h/thickness in (3).

these specimens as *Nudirostralina subtrinodosi* Yang and Xu, 1966. No description or discussion of these specimens were presented in the article (Chen, 1983). In addition, the external and internal features of these specimens are very different from those of *N. subtrinodosi* (see below). As a result, we re-identified these specimens.

Piarorhynchella mangyshlakensis Dagys, 1974, the type species of the genus *Piarorhynchella* Dagys, 1974, can be distinguished from *P. selongensis* n. sp. by the outline. The former species has a much wider shell (width significantly greater than length) than the latter species. The profile of *P. mangyshlakensis* is more convex than *P. selongensis* n. sp. *Piarorhynchella mangyshlakensis* shows a flat dorsal valve and a convex ventral valve. As for *P. selongensis* n. sp., its dorsal valve is slightly more convex than the ventral valve. *Piarorhynchella mangyshlakensis* has a distinct and high trapezoidal linguiform extension,

which is beveled at a high angle toward the anterior commissure. The height of the trapezoidal linguiform extension is equal to the thickness (Fig. 13). However, these features of linguiform extension are all different from *P. selongensis* n. sp. (Figs. 9.3, 9.4, 13). Compared to that in *P. selongensis* n. sp., *P. mangyshlakensis* has more-rounded plicae in the anterior. In addition, *P. mangyshlakensis* has three forms of plicae, namely 4/3 (Dagys, 1974, pl. 32, fig. 9, 7%), 3/2 (Dagys, 1974, pl. 32, fig. 8, 58%), and 2/1 (Dagys, 1974, pl. 32, fig. 10, 35%). However, *P. selongensis* n. sp. has only two types of plicae with similar proportions. In terms of internal structures, *P. mangyshlakensis* shows thick, massive, and narrow hinge plates (Fig. 13), including thickened and nearly horizontal outer hinge plates, and a narrow and deep septalium. However, *P. selongensis* n. sp. has much wider and thinner hinge plates (Figs. 10, 11, 13), horizontal or slightly oblique outer hinge plates, and a shallow and wide septalium. The crura of

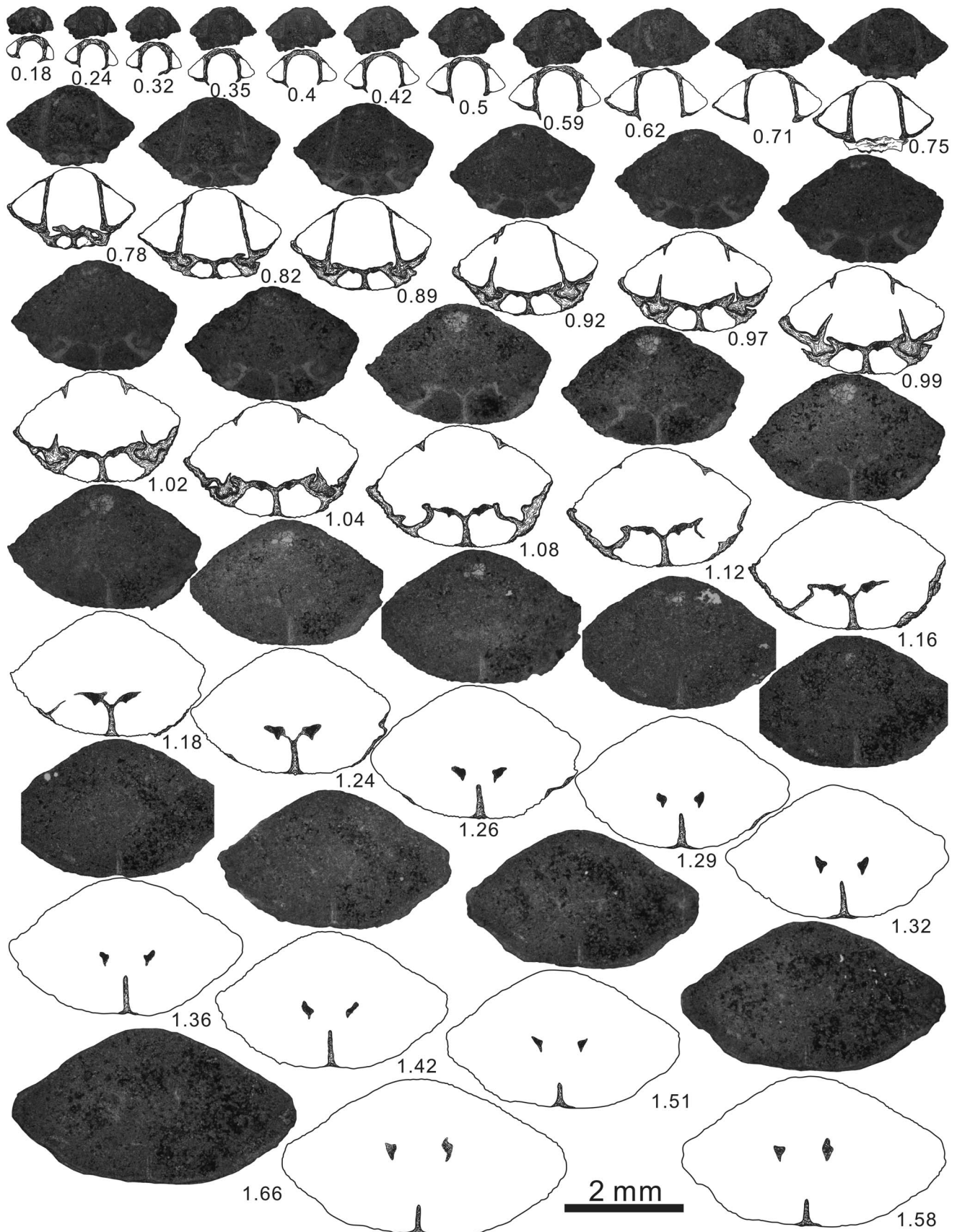


Figure 10. Serial sections of *Piarorhynchella selongensis* Wang and Chen n. sp. based on specimen SL-A-SS-002. The distance from the ventral beak to individual section is given in mm. Ventral valve upward. Sections continue in Figure 11.

P. mangyshlakensis were identified as calcariform by Dagens (1974). However, the distal ends of the crura present two lines inclined toward the symmetrical plane; no long hooks or expanded heads pointing to the dorsal valve were found. Thus, the crura of *P. mangyshlakensis* should be identified as raduliform (Fig. 13), that is, a short and strongly curved rod-like structure that projects toward the ventral valve. Therefore, the crura are the same in the two species.

Piarorhynchella trinodosi (Bittner, 1890), a widespread species in Europe (Bittner, 1890; Gaetani, 1969; Pálffy, 1988; Urošević et al., 1992), has wide intraspecific variation of the shell shapes (Bittner, 1890; Gaetani, 1969; Pálffy, 1988). Thus, comparison of the two species must consider ontogeny and intraspecific variation. Typical *P. trinodosi* shows high linguiform extensions (Bittner, 1890, pl. 32, figs. 17–28; Gaetani, 1969, pl. 34, figs. 1–7), which bevel at a high angle (sometimes approximately vertical) to the anterior commissure, forming a geniculate anterior portion that becomes the thickest part of the shell (Fig. 13). Meanwhile, *Piarorhynchella trinodosi* var. *latelinguata* (Bittner, 1890) and *Piarorhynchella trinodosi* cf. *toblochensis* (Bittner, 1890) have low and wide linguiform extensions (Bittner, 1890, pl. 32, figs. 29–32). However, nearly all mature specimens of *P. selongensis* n. sp. have less-developed linguiform extensions (Figs. 13, 9.3, 9.4). Because of intraspecific variation, *P. trinodosi* has a biconvex to geniculate biconvex profile. Nevertheless, the profile of *P. selongensis* n. sp. is only biconvex. The dominant types of plicae distribution of these two species are different. Two/one is the dominant form in Italian (70–98%, Gaetani, 1969), Alpine, and Hungarian specimens of *P. trinodosi* (Bittner, 1890). However, the two types of *P. selongensis* n. sp. have balanced proportions. *Piarorhynchella trinodosi* and *P. selongensis* n. sp. show significant differences in terms of ontogeny. The growth pattern of *P. trinodosi* attests to an ‘early maturity.’ Many structures already exist in most juvenile specimens, including the convex ventral valve, distinct linguiform extension (the height of the linguiform extension is approximately equal to the maximum thickness), an obvious sulcus, and a fold (Bittner, 1890, pl. 32, figs. 17–20, 24, 33; Gaetani, 1969; our personal collections). However, the juvenile specimens of *P. selongensis* n. sp. have a weak sulcus and fold or only have a low linguiform extension (Figs. 4, 7). The growth process of plicae is also different between two species. In juvenile of *P. selongensis* n. sp., the middle plica is smaller and lower than others because of the existence of a narrow sulcus in the middle of the dorsal valve (Figs. 4–6). However, in *P. trinodosi*, there is no sulcus on the dorsal valve, so the three plicae are of different sizes with the middle one always larger and higher than the other two (Bittner, 1890, pl. 32, figs. 28, 29, 31; Gaetani, 1969, pl. 34, fig. 3). It should be noted that the development of the lateral plicae of *P. trinodosi* is not consistent between original description (very weak, only pronounced in shell margin; Bittner, 1890, p. 14–15) and plates (long and distinct in lateral flanks; Bittner, 1890, pl. 32, figs. 17, 19–23, 25–28, 34). According to Gaetani (1969, p. 500, pl. 34, figs. 1–7), in combination with our personal specimens (collected in the same location), it was found that the lateral plicae were indeed very weak, and most specimens had only one real plica on the lateral shell surface next to the sulcus and fold on each

side. Therefore, the lateral plicae in these two species share the same features.

Piarorhynchella triassica (Girty, 1927), a common species from the western USA (Girty, 1927; Alexander, 1977; Perry and Chatterton, 1979), is elongate in comparison to *P. selongensis* n. sp. *P. selongensis* n. sp. is only slightly elongate in small shells, but becomes wider than long in larger shells (Figs. 4–6, 8.1). In profile, *P. triassica* is slightly to strongly dorsibiconvex, and the thickest part is located at the anterior of the shell. Nevertheless, *P. selongensis* n. sp. is biconvex, and the maximum thickness of *P. selongensis* n. sp. is situated in the middle of the shell. The characteristics of linguiform extension have obvious differences between the two species (Figs. 9.3, 9.4, 13). *P. triassica* has a long and high trapezoidal linguiform extension, which bevels at a high angle to the anterior commissure. The height of the linguiform extension is approximately equal to the thickness (Fig. 13). *P. triassica* always shows a narrow, high, and strongly inclined fold, both sides of which are strongly tilted. However, *P. selongensis* n. sp. has a wide and low dorsal fold. In light of the description by Perry and Chatterton (1979), *P. triassica* (1–3 plicae on the ventral sulcus and 2–4 plicae on the dorsal fold) has more plicae than *P. selongensis* n. sp. (1–2 plicae on the dorsal sulcus and 2–3 plicae on the ventral valve).

Piarorhynchella tazawai Popov in Popov and Zakharov, 2017 (9–14 mm long, 15 mm wide), which was first identified by Popov and Zakharov (2017), is larger than *P. selongensis* n. sp. (10.06 mm long, 11.21 mm wide). *P. tazawai* is elongate in comparison to *P. selongensis* n. sp. Length of adults of *P. selongensis* n. sp. is usually less than the width. The fold and sulcus of *P. tazawai* start from two-thirds of the length, and the top of the fold on the dorsal valve is relatively flat. However, the fold and sulcus of *P. selongensis* n. sp. start from the middle of the shell. Moreover, *P. tazawai* has more plicae than *P. selongensis* n. sp. (Fig. 13): *P. tazawai* has 1–6 plicae on the ventral sulcus, 2–7 on the dorsal fold, 1–3 obvious plicae on the lateral shell margin, and 1–2 bends found only on the lateral commissure. *P. tazawai* has a rounded submesothyrid foramen. However, *P. selongensis* n. sp. has an oval or rounded-triangle-shaped hypothryid foramen. In terms of the internal structures, the hinge teeth of *P. tazawai* are weaker than those of *P. selongensis* n. sp. (Fig. 13). Popov in Popov and Zakharov (2017) described *P. tazawai* as having a calcariform crura. However, based on the serial sections of *P. tazawai* (Popov in Popov and Zakharov, 2017, figs. 3, 4), the crura appears more raduliform, with the distal ends converging toward each other (Fig. 13).

Piarorhynchella kittli Gaetani in Grădinaru and Gaetani, 2019, is larger than *P. selongensis* n. sp., with a maximum length of 13.6 mm and maximum width of 16.3 mm (Grădinaru and Gaetani, 2019), while those of *P. selongensis* n. sp. are 10.06 mm and 11.21 mm, respectively. The linguiform extension of *P. kittli*, which is triangular or trapezoidal, bevels at a high angle to the anterior commissure. The height of the linguiform extension is less than or equal to the thickness because the dorsal fold is slightly recumbent in the anterior region (Fig. 13). However, *P. selongensis* n. sp. shows obvious differences with these aspects (Fig. 13). *P. kittli* seems to be characterized by asymmetrical development (Grădinaru and Gaetani, 2019, pl. 3, figs. B1–5, C1–5, D1–5, E1–5) and different sizes of plicae in the fold and sulcus (Grădinaru and Gaetani, 2019, pl. 3,

figs. C1-5, D1-5). However, very few specimens are asymmetric, and the plicae are always the same size on the fold and sulcus of *P. selongensis* n. sp. Due to the strong recrystallization in the shell, some of the internal structures of *P. kittli* are only roughly recognized with no detailed description (Grădinaru and Gaetani, 2019). Therefore, it is difficult to compare them to *P. selongensis* n. sp.

?*Piarorhynchella griesbachi* (Bittner, 1899a) seems to have more variation in outline, from subpentagonal (Bittner, 1899a, pl. 2, figs. 1, 2, 6) to elongated subpentagonal (Bittner, 1899a, pl. 2, figs. 3–5), than *P. selongensis* n. sp. (Fig. 13). In addition, there are 1–3 plicae on the ventral sulcus and 2–4 plicae on the dorsal valve, while *P. selongensis* n. sp. has at most two plicae on the ventral sulcus and three on the dorsal valve. Moreover, ?*P. griesbachi* has more distinct plicae on the fold and sulcus than *P. selongensis* n. sp. (Fig. 13). Because the serial sections of ?*P. griesbachi* originally published by Bittner (1899a) have not been studied, the internal structures of this species cannot be compared with *P. selongensis* n. sp. In addition, another species, ?*Piarorhynchella dieneri* (Bittner, 1899a), which was also collected in India, has some features in common with *P. selongensis* n. sp. However, ?*P. griesbachi* and ?*P. dieneri* should be represented as different ontogenetic stages of the same species (Gaetani et al., 2018).

Nudirostralina subtrinodosi Yang and Xu, 1966 (maximum length and width: 10.98 mm and 14.26 mm, respectively; Guo et al., 2019) is larger than *P. selongensis* n. sp. (maximum length and width: 10.06 mm and 11.21 mm, respectively). *N. subtrinodosi* is strongly dorsibiconvex in profile, while *P. selongensis* n. sp. is biconvex. *N. subtrinodosi* has a rather high and distinct linguiform extension, which is beveled toward the anterior commissure at a high angle, and the height is equal to or slightly less than the maximum thickness (Fig. 13). Therefore, the dorsal valve has a high and obvious fold corresponding to the linguiform extension. However, there are features that exhibit apparent differences from *P. selongensis* n. sp. (Fig. 13). *N. subtrinodosi* has more distinct and strong plicae (both on the sulcus and fold and lateral flanks) than *P. selongensis* n. sp. (Fig. 13). The plicae of *N. subtrinodosi* originate at the posterior or at two-thirds of the length. However, the plicae of *P. selongensis* n. sp. start from one-third to one-quarter of the length. In terms of the internal structures, the hinge teeth of *P. selongensis* n. sp. are stronger than those of *N. subtrinodosi* (Fig. 13). The crura of *N. subtrinodosi* are either canaliform or calcariform (Guo et al., 2019, fig. 8), while the crura of *P. selongensis* n. sp. might be treated as raduliform (Fig. 13). It should be noted that Guo et al. (2019) considered *Piarorhynchella* Dagys, 1974, and *Nudirostralina* Yang and Xu, 1966, to be essentially the same. However, by studying a large number of specimens of *P. selongensis* n. sp. (Figs. 4–12) and comprehensively reviewing the relevant literature for each species of *Piarorhynchella*, as well as taking into account ontogenetic characteristics and intraspecific variation, we found that all species of *Piarorhynchella* have the following stable characteristics (Fig. 13): (1) the length of plicae on the fold and sulcus is usually less than half of the length; (2) the plicae on the lateral flanks are weaker and shorter than the plicae on the fold and sulcus; (3) the dorsal valve has a long, massive median septum; and (4) the crura is raduliform. However, as mentioned above, the

distribution of the plicae, the development of lateral plicae, fold and sulcus, and the type of crura of *N. subtrinodosi* show obvious differences with these common features of *Piarorhynchella* (Fig. 13). Based on this evidence, we consider *Nudirostralina* (with *N. subtrinodosi* as a type species) and *Piarorhynchella* to be two different genera, but they are closely related in their evolution.

Order Athyrida Boucot, Johnson, and Staton, 1964
Suborder Retziidina Boucot, Johnson, and Staton, 1964
Superfamily Retzioidea Waagen, 1883
Family Neoretziidae Dagys, 1972
Subfamily Hustedinae Grunt, 1986
Genus *Schwagerispira* Dagys, 1972

Type species.—*Retzia schwageri* Bittner, 1890; Köveskál and Sintwag, North Alpine; Anisian.

Schwagerispira cheni Wang and Chen new species
Figures 14–17

Holotype.—Specimen SL-B-029 (Fig. 15.51–15.55), from the Early Triassic Kangshare Formation in the Selong section in southern Tibet, China.

Paratypes.—Specimens SL-B-028 (Fig. 15.46–15.50) and SL-B-027 (Fig. 15.41–15.45), from the Early Triassic Kangshare Formation in the Selong section in southern Tibet, China.

Diagnosis.—Small size, generally elliptical in outline, equibiconvex in profile, anterior commissure rectimarginate, dorsal median sulcus very weak, shallow, and only developed at the anterior region. Shells bear 9–14 costae, median costa on the dorsal sulcus slightly weaker and wider than the adjacent two costae. Width of interspace equal to width of costae. Bottom of the interspace flat. Pedicle collar developed, dental plates absent, cardinal flanges very thick and project toward the ventral valve, hinge plates thick, and the middle portion arched toward the ventral valve.

Occurrence.—Kangshare Formation of early Smithian, Selong section, southern Tibet, China.

Description.—Shell generally elliptical (a small number of specimens subcircular) in outline. Small size (2.01–9.61 mm long, 1.81–8.26 mm wide); length obviously larger than width; maximum width located at two-thirds of length anteriorly. Equibiconvex in profile, 0.85–5.73 mm thick; maximum thickness reached in the middle of the shell. Lateral margin nearly straight to slightly curved; anterior margin straight. Hinge line short and curved, much shorter than the maximum width. Dorsal sulcus very weak, only appearing at anterior region. Anterior commissure rectimarginate. Shell surface entirely covered by round costae, without distinct concentric growth lines.

Ventral valve mildly convex, maximum convexity approximately in the middle of the valve. Umbo mildly curved, middle part flat, anterior slightly to mildly bent. Apical angles 74–106°. Beak distinct, slightly incurved. Beak ridges round. Small

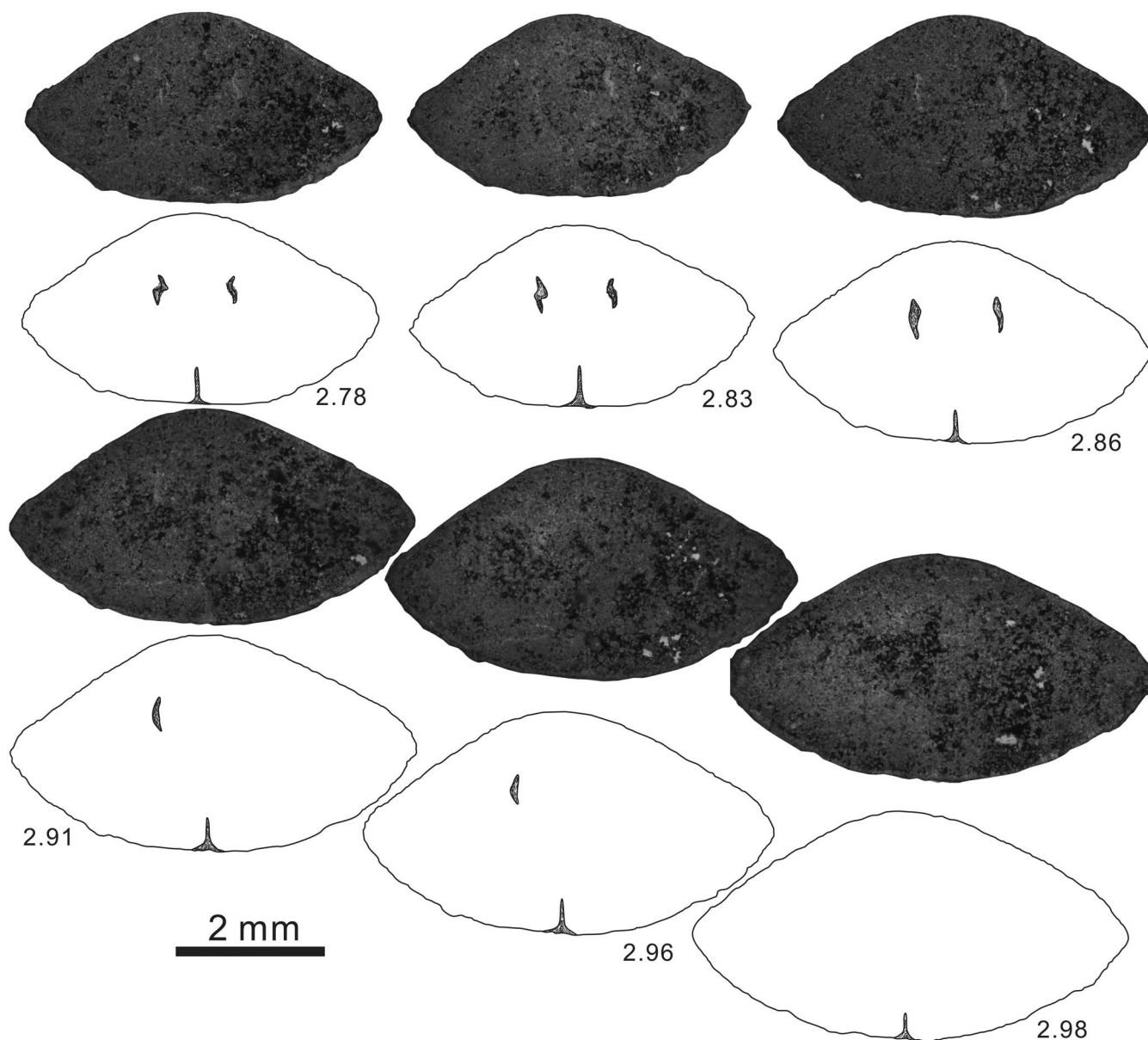


Figure 11. Serial sections of *Piatorhynchella selongensis* Wang and Chen n. sp. based on specimen SL-A-SS-002. Sections continued from Figure 10.

foramen permesothyrid, oval to circular in shape. Interarea apsacline, high and distinct. Deltoidal plates divided.

Dorsal valve mildly convex, maximum convexity approximately at mid-length. Umbo strongly curved, middle part flat, anterior slightly to mildly bent. Extremely shallow and narrow sulcus begins at middle to anterior of ventral valve, indistinct. One costa on the sulcus.

Shell surface bears straight and simple costae, with no bifurcation and extending anteriorly from the beak. Costae rounded, with the tops flat, and the sides strongly inclined. Interspace between two adjacent costae shallow, with flat bottom. Width of the interspace is equal to width of the costa. Three types of costae arrangement appear: 10 costae on the ventral valve and nine costae on the dorsal valve (10/9, 12%), 12 costae on the ventral valve and 11 costae on the dorsal valve (12/11, 68%), and 14 costae on the ventral valve and 13 costae on the

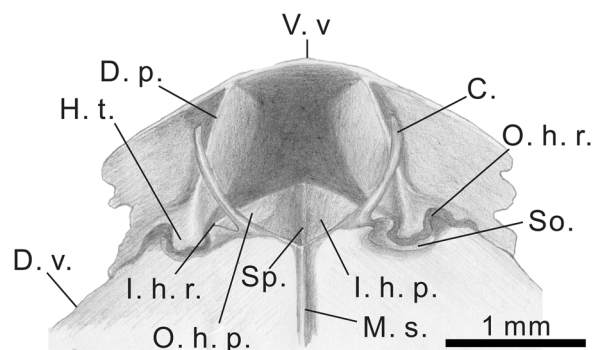


Figure 12. Reconstructed dorsal internal view of *Piatorhynchella selongensis* Wang and Chen n. sp. based on the serial sections in Figures 10, 11. Abbreviations: C. = Crura; D. p. = dental plate; D. v. = dorsal valve; H. t. = hinge teeth; I. h. p. = inner hinge plate; I. h. r. = inner hinge ridge; M. s. = median septum; O. h. p. = outer hinge plate; O. h. r. = outer hinge ridge; So. = socket; Sp. = septalium; V. v. = ventral valve.

Species	Features	Size	Outline	Profile	Linguliform extension	Number and strength of plicae		Hinge teeth	Outer hinge plates	Septalium	Median septum	Crura
						Fold/sulcus	Lateral flanks					
<i>P. selongensis</i> n. sp.		small		biconvex		3/2, 2/1 1/3-1/4 of shell length	1 or 2 short and weak	strong	 thin and wide	shallow and wide	long, $\geq \frac{1}{2}$ of shell length	 raduliform
<i>P. mangyshlakensis</i> Dagys, 1974		small		biconvex to planoconvex		4/3, 3/2, 2/1 1/2 of shell length	1 or 2 short and weak	strong	 thick and narrow	shallow and narrow	long, $\geq \frac{1}{2}$ of shell length	 raduliform
<i>P. trinodosi</i> (Bittner, 1890)		small		strongly biconvex		3/2, 2/1 1/2-1/3 of shell length	1 or 2 short and weak	strong	 thin and wide	shallow and wide	long, $\geq \frac{1}{2}$ of shell length	 raduliform
<i>P. triassica</i> (Girty, 1927)		small		strongly dorsibiconvex		?4/3, 3/2, 2/1 1/2 of shell length	1, 2 or 3 short and weak	moderate strong	 thin and wide	shallow and wide	long, $\geq \frac{1}{2}$ of shell length	 raduliform
<i>P. tazawai</i> Popov in Popov and Zakharov, 2017		medium		biconvex		5/4, 4/3, 3/2, 1/2-1/3 of shell length	1, 2 or 3 short and distinct	weak	 thin and wide	shallow and wide	long, $\geq \frac{1}{2}$ of shell length	 raduliform
<i>P. kittli</i> Gaetani in Grádinaru and Gaetani, 2019		medium		biconvex		3/2, 2/1 1/2 of shell length	2 or 3 short or long and distinct	unknown	unknown	unknown	unknown	unknown
<i>N. subtrinodosi</i> Yang and Xu, 1966		medium		strongly dorsibiconvex		3/2, 2/1 $\geq 2/3$ of shell length	2 or 3 long and distinct	weak	 thin and wide	shallow and wide	long, $\frac{1}{2}$ of shell length	 canaliform or calcariform
? <i>P. griesbachi</i> (Bittner, 1899a)		medium		biconvex		4/3, 3/2, 2/1 1/2 of shell length	3 or 4 short and distinct	unknown	unknown	unknown	unknown	unknown

Figure 13. Comparison of the main external and internal features in all the species of *Piarorhynchella*. The figures of crura are shown by the distal ends in serial sections.

dorsal valve (14/13, 20%). Middle costa on the shallow and narrow dorsal sulcus depressed, and with quite flat top. Development of the middle costa weaker than that of adjacent costae. Width of the middle costa larger than that of other costae, especially at the anterior region. Strength and width of the costae on both sides of the middle costa decrease slowly to the posterior region. Middle interspace on the ventral valve much wider than that of other interspaces. Strength and width of the costae on both sides of the middle interspaces also decrease slowly towards the postero-lateral region.

Pedicle collar in the ventral valve well developed, connects to the deltidial plates. Dental plates absent. Blunt hinge teeth elongate transversely and parallel to the hinge axis. Cardinal flanges in the dorsal valve highly developed, extend from inner socket ridges perpendicular to the hinge axis and project strongly to the ventral valve. Lumpy cardinal flanges extend from the cardinal plate and approach the ventral valve. Hinge plates thick, and middle portion arched to the ventral shell, forming cusps. Median septum thin and relatively high. Spiralia and jugum unknown.

Etymology.—In honor of the Chinese paleontologist Yongming Chen, who studied the Early and Middle Triassic brachiopods in Tulong in southern Tibet, China.

Material.—A total of 181 complete specimens collected from the Early Triassic Kangshare Formation. Of these, four specimens were sectioned (SL-B-SS-001, SL-B-SS-002 [Fig. 17], SL-B-SS-003, SL-B-SS-004) and 29 selected specimens were photographed.

Remarks.—*Schwagerispira schwageri* (Bittner, 1890), the type species of the genus *Schwagerispira* Dagys, 1972, has a different number of costae than *S. cheni* n. sp. *S. schwageri* has two types costae distributions: 6/7 (Bittner, 1890, pl. 36, figs. 1, 2, 4; Dagys, 1974, pl. 42, fig. 8; Pálffy, 2003, pl. Br-I, fig. 3) and 10/11 (Bittner, 1890, pl. 36, fig. 3). The beak of *S. schwageri* is much stronger and higher than that of *S. cheni* n. sp. (Bittner, 1890, pl. 36, figs. 1, 3). The costae of *S. schwageri* are subangular and appear subtriangular in cross-sections, while those of *S. cheni* n. sp. are rounded and appear semi-circular in cross-sections. In addition, the interspaces between two adjacent costae of *S. schwageri* are always narrower than the width of the costae. The bottom of the interspace is V-shaped (Fig. 18). Nevertheless, these features are completely different than *S. cheni* n. sp. (Fig. 18). Bittner (1890) noted that *S. schwageri* has a slightly recessed middle costa on the dorsal valve (Bittner, 1890, pl. 36, figs. 1, 3), and the width of the middle costa is larger than or equal to

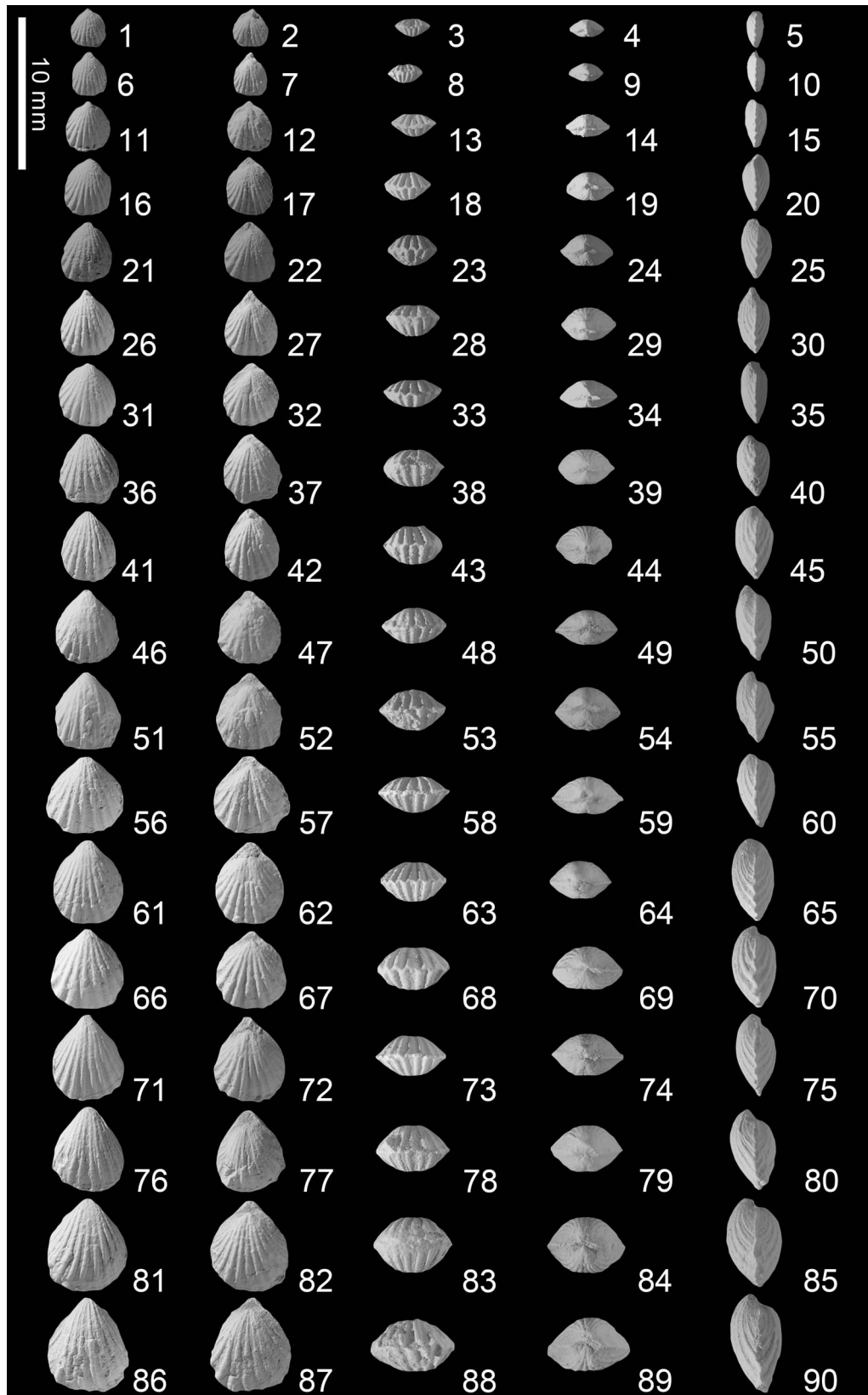


Figure 14. *Schwagerispira cheni* Wang and Chen n. sp. from the Kangshare Formation of Selong section, southern Tibet. For each shell we present ventral, dorsal, anterior, posterior, and lateral views. (1–5) SL-B-001; (6–10) SL-B-002; (11–15) SL-B-003; (16–20) SL-B-004; (21–25) SL-B-005; (26–30) SL-B-006; (31–35) SL-B-007; (36–40) SL-B-008; (41–45) SL-B-009; (46–50) SL-B-010; (51–55) SL-B-011; (56–60) SL-B-012; (61–65) SL-B-013; (66–70) SL-B-014; (71–75) SL-B-015; (76–80) SL-B-016; (81–85) SL-B-017; (86–90) SL-B-018.

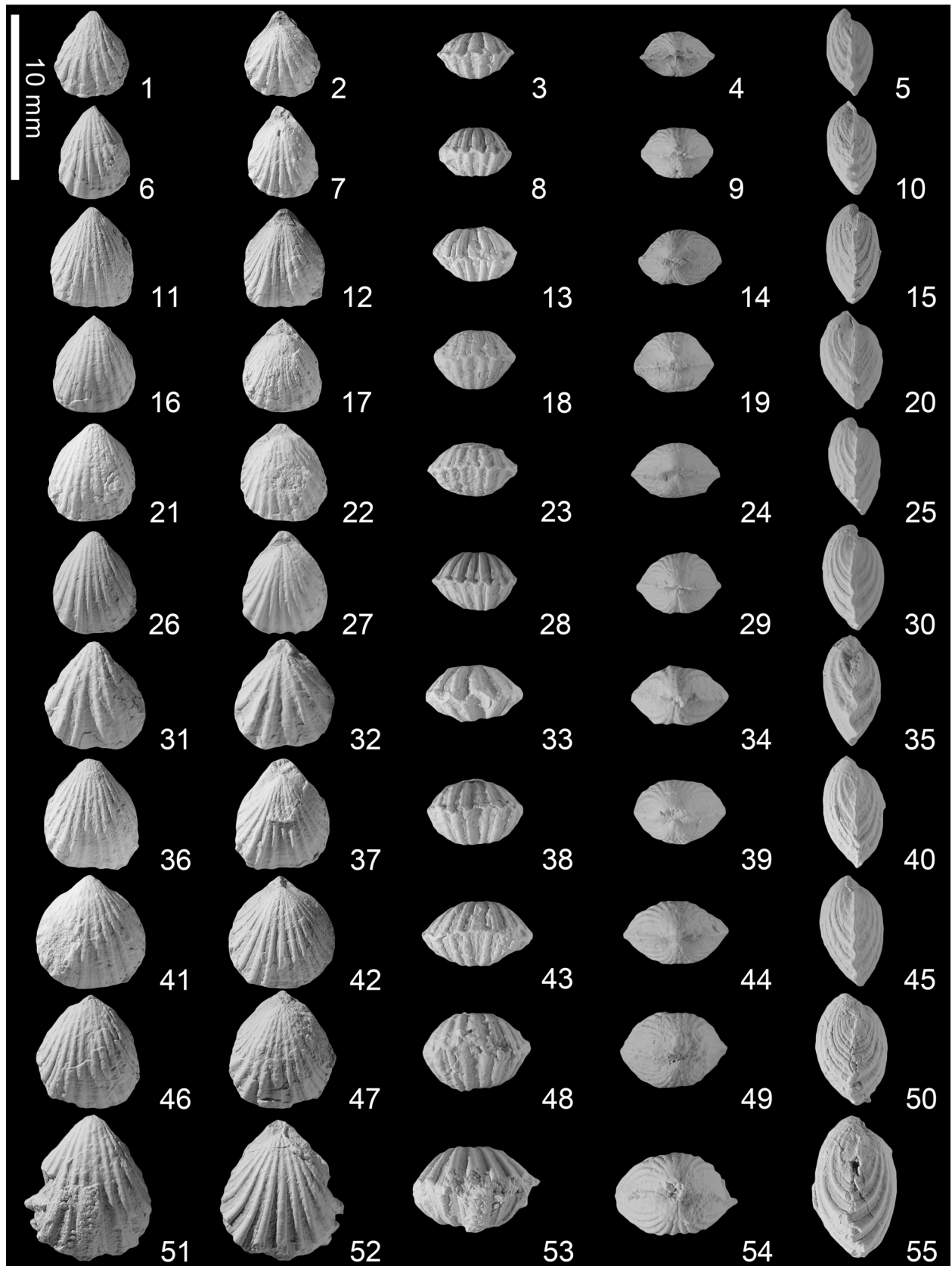


Figure 15. *Schwagerispira cheni* Wang and Chen n. sp. from the Kangshare Formation of Selong section, southern Tibet. For each shell we present ventral, dorsal, anterior, posterior, and lateral views. (1–5) SL-B-019; (6–10) SL-B-020; (11–15) SL-B-021; (16–20) SL-B-022; (21–25) SL-B-023; (26–30) SL-B-024; (31–35) SL-B-025; (36–40) SL-B-026; (41–45) paratype SL-B-027; (46–50) paratype SL-B-028; (51–55) holotype SL-B-029.

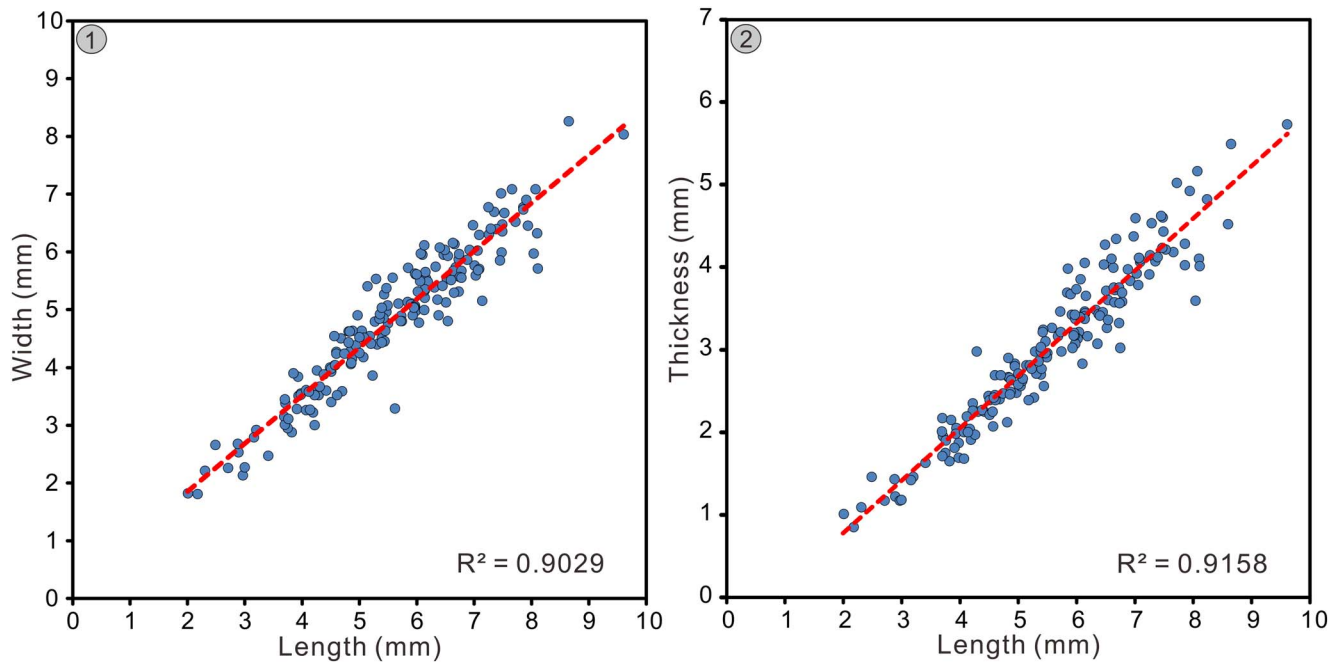


Figure 16. (1) Scatter plot of length/width of 181 articulated shells of *Schwagerispira cheni* Wang and Chen n. sp. (2) Scatter plot of length/thickness of the same. The red dotted line represents the trend line.

that of other costae. However, these features are absent from other specimens collected by Dagens (1972, 1974) and Pálffy (2003). Therefore, it may be different than *S. cheni* n. sp. *S. schwageri* has two lobed cardinal flanges extending from the cardinal plate (Fig. 18). However, *S. cheni* n. sp. has massive cardinal flanges stretching from the cardinal plate (Figs. 17, 18).

Schwagerispira fuchsi (Koken, 1900) was first collected in southwestern China. This species also has been reported by Sun and Ye (1982) in northwestern China. However, *S. fuchsi* lacks a distinct dorsal sulcus and a recessed, narrow middle costa (Sun and Ye, 1982, pl. 3, figs. 5–8). Therefore, these specimens might not represent typical *S. fuchsi*. *S. fuchsi* has subangular costae that are subtriangular in cross-sections, while *S. cheni* n. sp. has rounded costae that are semi-circular in cross-sections. The dorsal sulcus of *S. fuchsi* is more distinct than *S. cheni* n. sp. The median costa, which is located in the dorsal sulcus, has opposite development between two species. The median costa of *S. fuchsi* is weaker, lower, and narrower than the adjacent costae. The two widest and most-developed costae are situated alongside the dorsal sulcus (Fig. 18). However, the middle costa of *S. cheni* n. sp. is wider than that of other costae. *S. fuchsi* has V-shaped interspaces between two adjacent costae. However, the bottom of the interspace between two adjacent costae of *S. cheni* n. sp. is very flat. Moreover, the hinge plates of *S. cheni* n. sp. are much thicker than that of *S. fuchsi* (Fig. 18).

The outline of *Schwagerispira subcircularis* (Yang and Xu, 1966) is subcircular, whereas *S. cheni* n. sp. shows a generally elliptical outline (Fig. 18). There is no sulcus on the dorsal valve of *S. subcircularis* (Yang and Xu, 1966). However, *S. cheni* n. sp. has a dorsal sulcus. The costae of *S. subcircularis* are subangular, and the widths of the V-shaped interspaces are less than the widths of the costae. Nevertheless, *S. cheni* n. sp.

has rounded costae, the widths of which are equal to those of the interspaces. The bottoms of the interspaces are flat. Because serial sections of *S. subcircularis* have never been studied, their internal structures cannot be compared with *S. cheni* n. sp.

Schwagerispira pinguis Sun and Ye, 1982, has a rounded triangular outline (Fig. 18), whereas the outline of *S. cheni* n. sp. is a generally elliptical shape. The shell convexity of *S. pinguis* is slightly greater than that of *S. cheni* n. sp. *S. pinguis* has no sulcus on the dorsal valve. The size and development of the middle costa on the dorsal valve are the same as those of the adjacent costae. However, *S. cheni* n. sp. has a dorsal sulcus. The dorsal middle costa is wider than the adjacent costae. Interiorly, *S. pinguis* has thin hinge plates and a strong dorsal median septum (Fig. 18), while *S. cheni* n. sp. has very thick hinge plates and a thin dorsal median septum (Figs. 17, 18).

Schwagerispira sichuanensis Liao and Sun, 1974, has a much higher and longer ventral beak than that of *S. cheni* n. sp. The features of costae and interspace are completely different between the two species. The costae of *S. sichuanensis* are subangular and subtriangular in cross section. The width of the V-shaped interspace between two adjacent costae is narrower than the width of the costa. *S. sichuanensis* has no sulcus on the dorsal valve. Therefore, the middle costa on the dorsal valve shows no difference from adjacent costae. These features also show distinct differences with *S. cheni* n. sp. In the internal structures, *S. sichuanensis* has thick and two-lobed cardinal flanges extending from the cardinal plate (Fig. 18), while *S. cheni* n. sp. has rounded cardinal flanges stretching from the cardinal plate (Figs. 17, 18).

Both *Schwagerispira fastosa* (Bittner, 1890) and *S. cheni* n. sp. are generally elliptical, but the former shows significant varieties in outline from elongated subpentagonal to generally

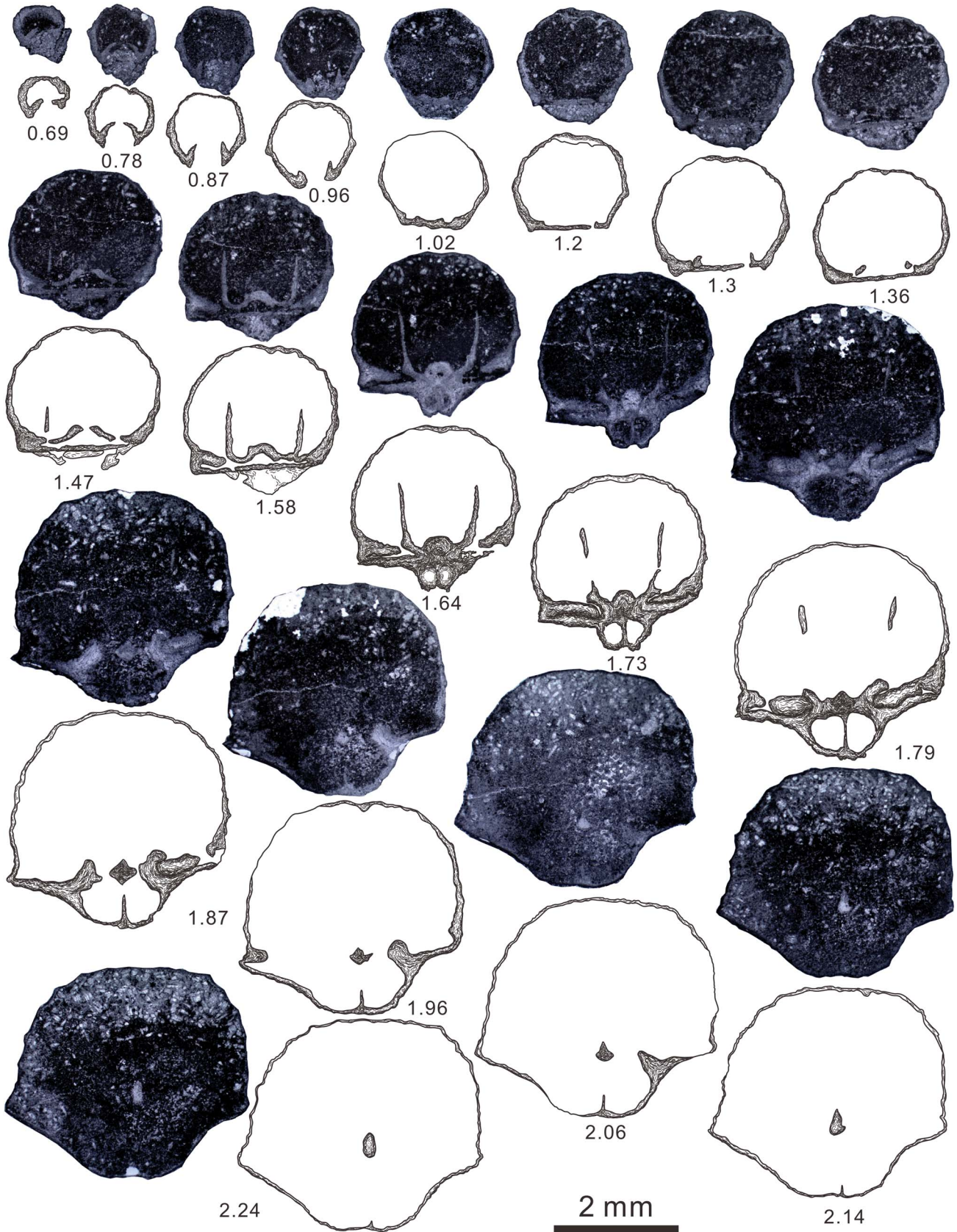


Figure 17. Serial sections of *Schwagerispira cheni* Wang and Chen n. sp. based on specimen SL-B-SS-002. The distance from the ventral beak to individual section is given in mm. Ventral valve upward.

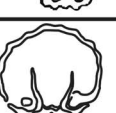
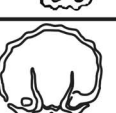
Features Species	Outline	Dorsal sulcus	Costae	Width and strength of middle costae in dorsal valve	Interspaces between costae		Cardinal flanges	Hinge plates	Median septum
					Width	Shape			
<i>S. cheni</i> n. sp.	generally elliptical	very weak and shallow	rounded	weaker and wider than adjacent costae	=width of costae	flat bottom			
<i>S. schwageri</i> (Bittner, 1890)	generally elliptical	without	subangular	weaker than or equal to adjacent costae	<width of costae	V-shaped			
<i>S. fuchsi</i> (Koken, 1900)	generally elliptical	shallow and narrow	subangular	weaker, lower and narrower than adjacent costae	<width of costae	V-shaped			
<i>S. pinguis</i> Sun and Ye, 1982	rounded triangular	without	rounded	equal to adjacent costae	=width of costae	flat bottom			
<i>S. sichuanensis</i> Liao and Sun, 1974	generally elliptical	without	subangular	equal to adjacent costae	<width of costae	V-shaped			
? <i>S. tulongensis</i> (Chen, 1983)	generally elliptical	without	rounded	equal to adjacent costae	=width of costae	slightly convex bottom			
<i>S. subcircularis</i> (Yang and Xu, 1966)	subcircular	without	subangular	equal to adjacent costae	<width of costae	V-shaped	unknown	unknown	unknown
<i>S. fastosa</i> (Bittner, 1890)	generally elliptical to elongated subpentagonal	indistinct or without	subangular	equal to adjacent costae	<width of costae	V-shaped	unknown	unknown	unknown

Figure 18. Comparison of the main external and internal features in all the species of *Schwagerispira*. The figures of crura show the distal ends in serial sections.

elliptical. The beak of *S. fastosa* is more distinct and higher than that of *S. cheni* n. sp. *S. fastosa* has a very indistinct sulcus on the dorsal valve, while *S. cheni* n. sp. has a narrow and shallow sulcus. According to the original description by Bittner (1890), the middle costa on the dorsal valve of *S. fastosa* is usually weaker and lower than or has the same development as the adjacent costae. However, these features were not observed in specimens collected from the other areas (Bittner, 1890, pl. 36, figs. 17–20; Jin and Fang, 1977, pl. 5, figs. 13–16; Jordan, 1993, pl. 2, fig. 7; Siblík, 1994, pl. 1, fig. 9; Siblík and Bryda, 2005, pl. 2, fig. 2). It seems that this feature is not stable in *S. fastosa*. Through the observation of specimens from different regions, we found that *S. fastosa* has subangular costae; the widths of interspaces are smaller than the widths of the costae and are V-shaped. These features stand in stark contrast to *S. cheni* n. sp. The internal structures of *S. fastosa* have not been studied.

?*Schwagerispira tulongensis* (Chen, 1983) has fewer costae than that does *S. cheni* n. sp. The bottom of the interspaces of ?*S. tulongensis* are slightly convex, while the bottom of the

interspaces of *S. cheni* n. sp. are flat. Based on the indistinct serial sections of ?*S. tulongensis*, the cardinal flanges and hinge plates seem very thin (Chen, 1983, fig. 4; Fig. 18). However, *S. cheni* n. sp. possesses very developed and thick cardinal flanges and hinge plates (Figs. 17, 18).

Order Terebratulida Waagen, 1883
Suborder Terebratulidina Muir-Wood, 1955
Superfamily Zeillerioidea Allan, 1940
Family Zeilleriidae Allan, 1940
Subfamily Zeilleriinae Allan, 1940
Genus *Selongthyris* Wang and Chen new genus

Type species.—*Selongthyris plana* Wang and Chen n. gen. n. sp., Kangshare Formation, Early Triassic, Selong section, southern Tibet, China.

Diagnosis.—Small size, shell flat, subcircular, elongate suboval to subpentagonal in outline, ventribiconvex in profile, without fold

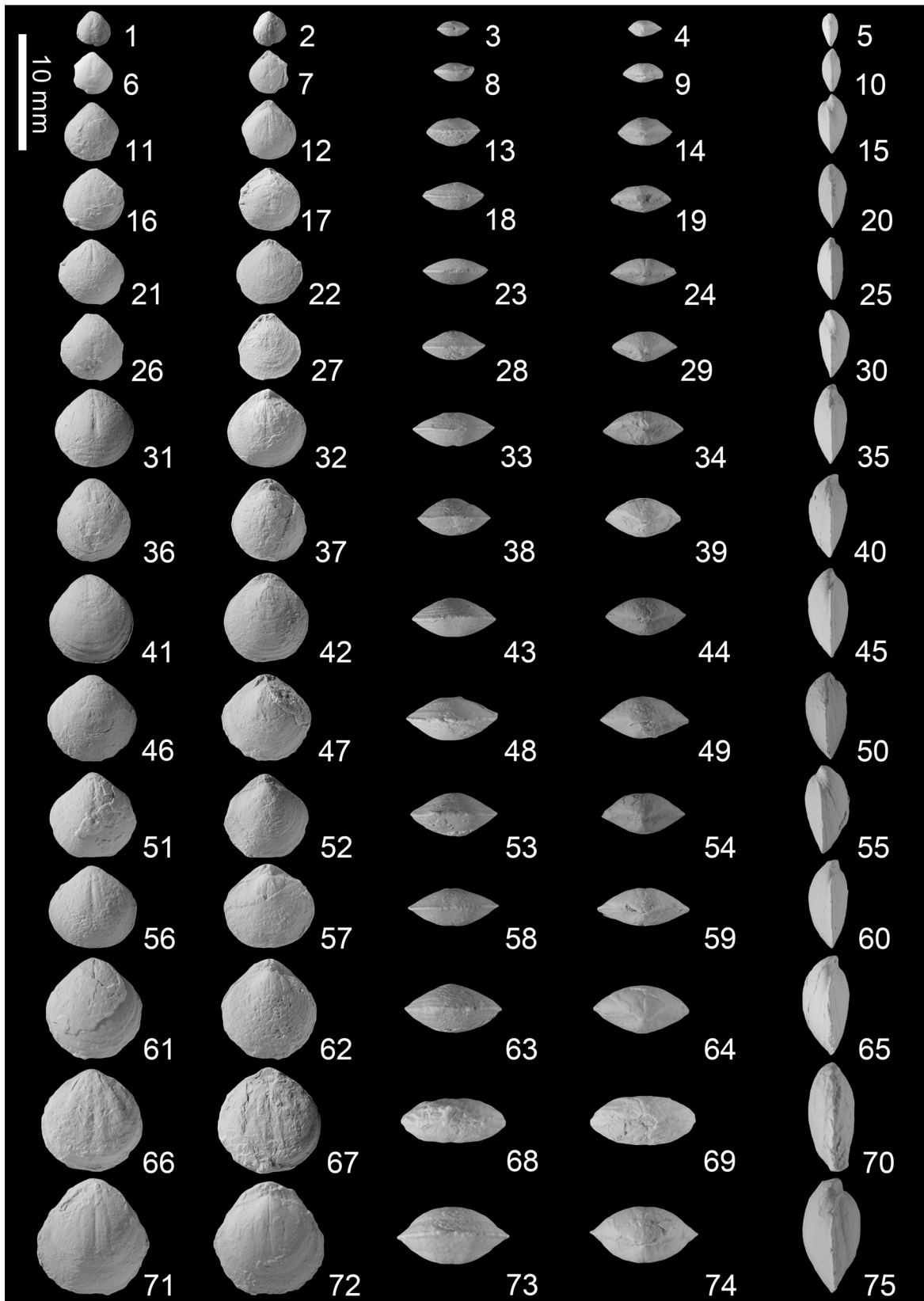


Figure 19. *Selongthyris plana* Wang and Chen n. gen. n. sp. from the Kangshare Formation of Selong section, southern Tibet. For each shell we present ventral, dorsal, anterior, posterior, and lateral views. (1–5) SL-C-001; (6–10) SL-C-002; (11–15) SL-C-003; (16–20) SL-C-004; (21–25) SL-C-005; (26–30) SL-C-006; (31–35) SL-C-007; (36–40) SL-C-008; (41–45) SL-C-009; (46–50) SL-C-010; (51–55) SL-C-011; (56–60) SL-C-012; (61–65) paratype SL-C-013; (66–70) paratype SL-C-014; (71–75) holotype SL-C-015.

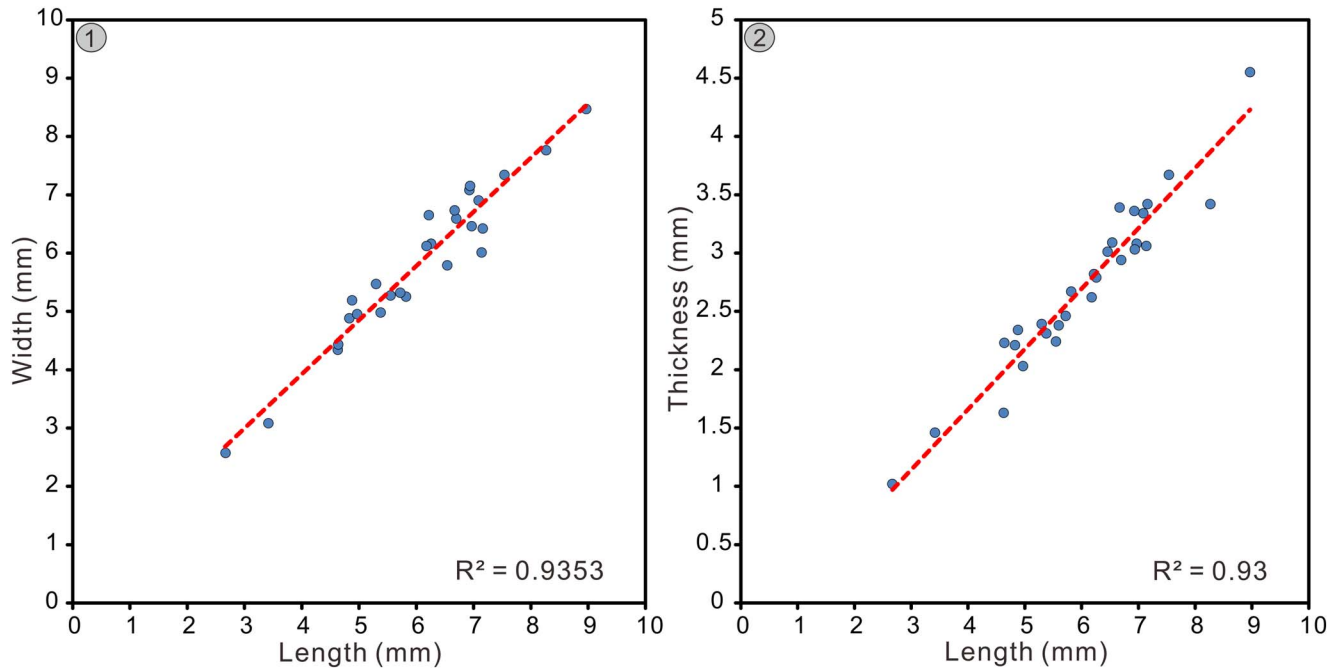


Figure 20. (1) Scatter plot of length/width of 181 articulated shells of *Selongthyris plana* Wang and Chen n. gen. n. sp. (2) Scatter plot of length/thickness of the same. The red dotted line represents the trend line.

and sulcus, anterior commissure rectimarginate, shell smooth without plicae. Ventral myophragm low and long. Dental plates absent. Hinge plates undivided. Septalium shallow and wide. Crural bases arise from the inner socket ridges and hinge plates stretch to the ventral valve. Loop long and delicate, teloform, descending lamellae slightly curved anteriorly, strongly convergent and closer each other, spine structures absent.

Occurrence.—Kangshare Formation of the early-late Smithian, Selong section, southern Tibet, China.

Etymology.—Named after the Selong section, and the Latin *thyris*, window or hole.

Remarks.—According to the diagnostic criteria, *Selongthyris* n. gen. is easily distinguished from most of the subfamily Zeilleriinae Allan, 1940. *Periallus* Hoover, 1979, is the most similar taxon to *Selongthyris* n. gen. in terms of the external features. However, the anterior commissure of *Periallus* ranges from rectimarginate, to uniplicate or paraplicate, whereas *Selongthyris* n. gen. only has a rectimarginate anterior commissure. There were obvious differences in the internal structures between the two genera mainly based on the absence of a low ventral myophragm in *Periallus*. In addition, *Periallus* has divided hinge plates, and its inner hinge plates are unstable and are sometimes absent entirely. The median septum and septalium are present or replaced by crural plates directly connected to the dorsal valve. Crural bases arise from the middle of the hinge plates and stretch to the dorsal valve. In addition, the descending lamellae converge anteriorly, but are separated widely. The whole dorsal surface of the descending lamellae is covered with many spines.

The Early Triassic *Obnixia* Hoover, 1979, and *Protogusarella* Perry and Chatterton, 1979, have a shallow sulcus and fold in the anterior region, and the anterior commissure is unisulcate. However, *Selongthyris* n. gen. does not develop a sulcus or fold on the shell; thus, it has a rectimarginate anterior commissure. The internal structures of *Selongthyris* n. gen. are quite different from those of the other two genera. There is no median septum or septalium in either *Obnixia* or *Protogusarella*. The crural bases stretch to the dorsal valve, and the descending lamellae converge anteriorly, but are wide separated. In addition, the loop of *Obnixia* has spines on the junction of the descending lamellae and ascending lamellae.

Selongthyris plana Wang and Chen new species
Figures 19–23

Holotype.—Specimen SL-C-015 (Fig. 19.71–19.75) from the Early Triassic Kangshare Formation in the Selong section in southern Tibet, China.

Paratypes.—Specimens SL-C-013 (Fig. 19.61–19.65) and SL-C-014 (Fig. 19.66–19.70) from the Early Triassic Kangshare Formation in the Selong section in southern Tibet, China.

Diagnosis.—Shell small and flat, subcircular, elongate suboval to subpentagonal in outline, ventribiconvex in profile, anterior commissure rectimarginate, shell surface without fold and sulcus, shell entirely smooth. Ventral myophragm low and long, dental plate thin but distinct, hinge teeth long. Dorsal valve with deep sockets, inner socket ridges thick, hinge plates undivided, crural bases arise from the junction of inner socket ridges and hinge plates, and stretch to the ventral valve, median

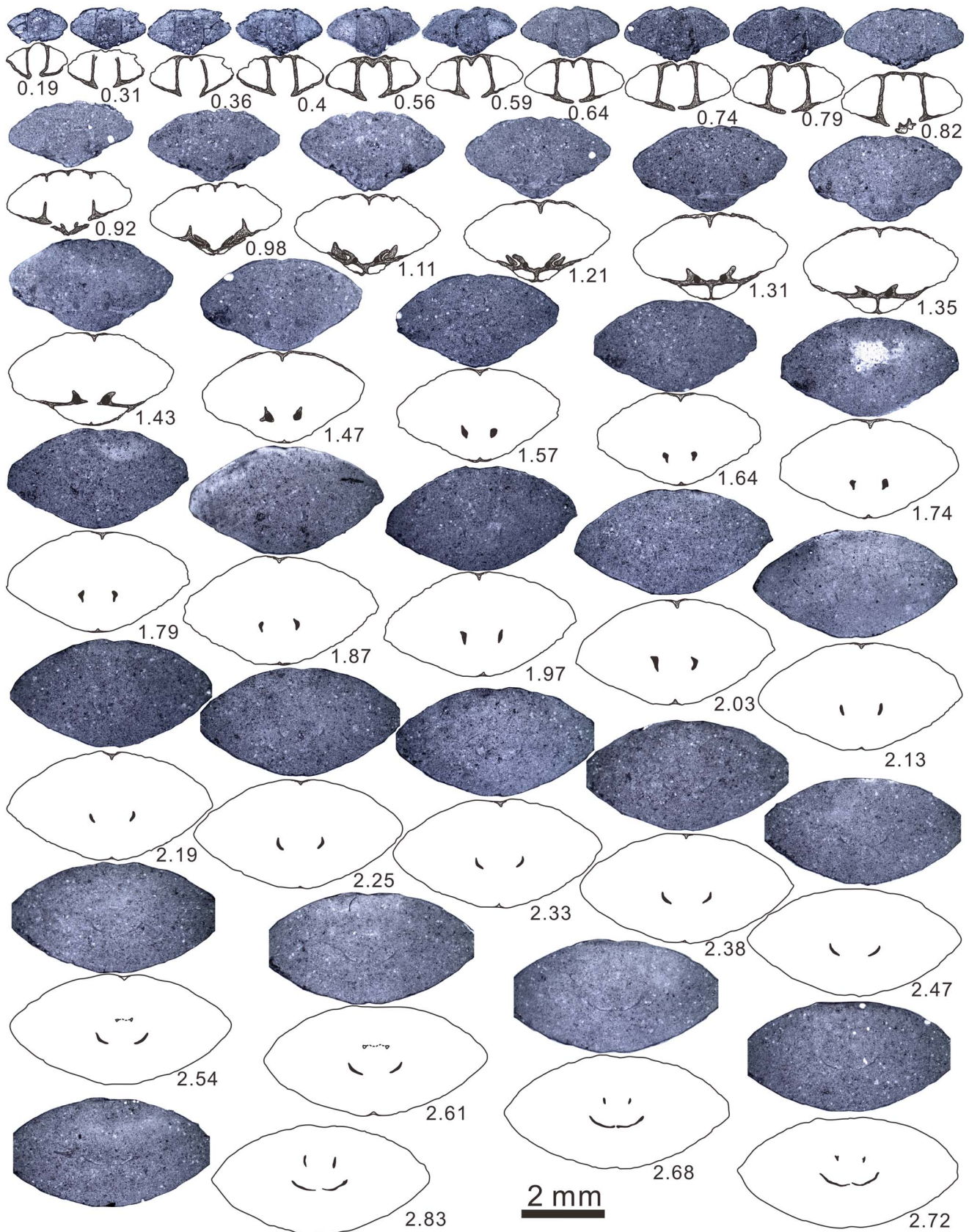


Figure 21. Serial sections of *Selongthyris plana* Wang and Chen n. gen. n. sp. based on specimen SL-C-SS-001. The distance from the ventral beak to individual section is given in mm. Ventral valve upward. Sections continue in [Figure 22](#).

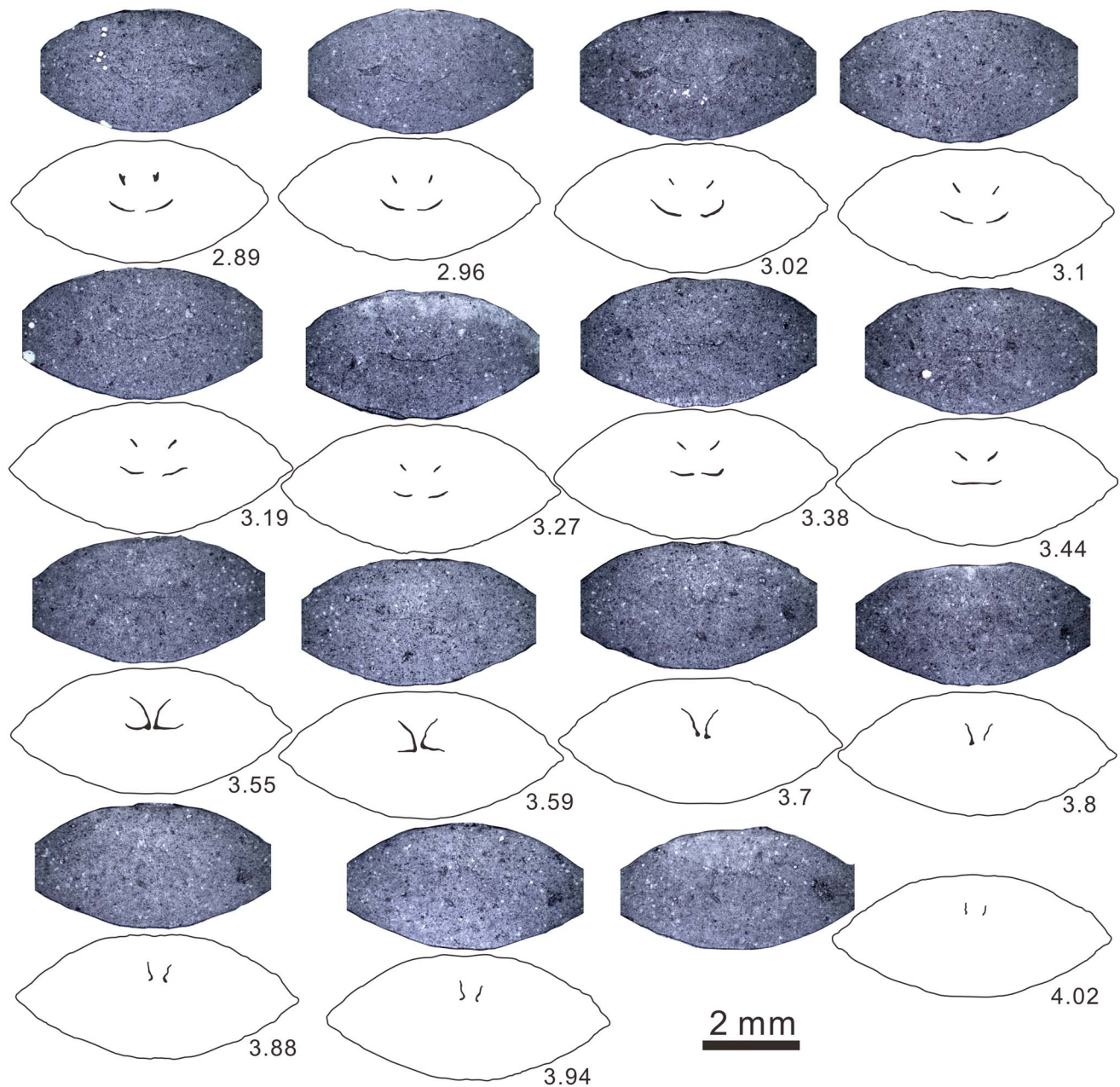


Figure 22. Serial sections of *Selongthyris plana* Wang and Chen n. gen. n. sp. based on specimen SL-C-SS-001. Sections continued from [Figure 21](#).

septum high, septalium shallow and wide. Loop telloform, long and delicate, descending lamella slightly curved anteriorly, strongly convergent, and closely approached, ascending lamellae extended relatively broadly. No spine structures on loop.

Occurrence.—Kangshare Formation of the early-late Smithian, Selong section, southern Tibet, China.

Description.—Subcircular, elongate suboval to subpentagonal in outline. Shell small, 2.67–8.97 mm long, 2.57–8.47 mm wide; length slightly larger than width, or equidimensional; maximum width at middle of the shell. Ventribiconvex (occasionally subequally biconvex) in profile; very flattened shell, 1.02–4.55 mm thick, maximum thickness located in middle to posterior

part of the shell. Postero-lateral margin straight; lateral margin rounded, strongly curved; anterior margin straight to slightly curved. Hinge line short and curved, much shorter than the maximum shell width. Anterior commissure rectimarginate, without ventral or dorsal fold and sulcus. Shell smooth, covered with concentric growth lines and lamellae in the anterior region.

Ventral valve gently convex, maximum convexity located approximately close to the umbonal region. Umbo mildly convex, middle part flat, anterior part extends forward and is slightly bent. Beak wide and short, slightly incurved, tangential to and slightly protrudes out of the commissure plane, apical angles 98–136°. Beak ridges round and straight. Interarea short but distinct, triangular in shape. Foramen mesothyrid small, oval or circular in shape; deltidial plates divided.

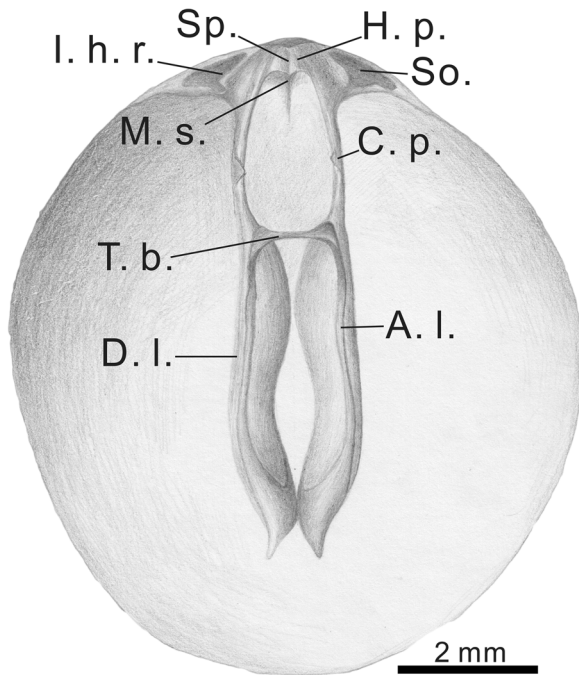


Figure 23. Reconstructed dorsal internal view of *Selongthyrus plana* Wang and Chen n. gen. n. sp. based on the serial sections in Figures 21 and 22. Abbreviations: A. l. = ascending lamellae; C. P. = crural process; D. l. = descending lamellae; H. p. = hinge plate; I. h. r. = inner hinge ridge; M. s. = median septum; So. = socket; Sp. = septalium; T. b. = transverse band.

Dorsal valve slightly convex, maximum convexity located at the umbonal region. Umbo strongly curved, middle and anterior part slightly bent forward with the same degree.

Ventral dental plates thin and straight, nearly parallel posteriorly and slightly converge anteriorly. Hinge teeth relatively strong and long, oblique to the plane of symmetry at $\sim 45^\circ$. Myophragm low and long up to half of length of shell in size. Pedicle collar unknown. Dorsal valve with deep sockets expands anterolaterally. Inner hinge ridges very developed and thick, posterodistally hooked, oblique to the plane of symmetry at $\sim 45^\circ$. Hinge plates thin, undivided, tilt toward the plane of symmetry at $\sim 45^\circ$. Median septum thick and low, extending approximately one-third of the length of the dorsal valve, and connects to hinge plates forming very shallow and wide septalium. Cardinal process undeveloped. Crural bases large, very distinct, oval to circular in shape, arising from the junction of inner socket ridges and hinge plates, and stretch to the ventral valve. Loop teliform, long and delicate, commonly about two-thirds of the length of the dorsal valve; descending lamellae slightly curved anteriorly, strongly convergent, and closely approached, while the ascending lamellae are relatively broadly extended. Crural process short, width slightly larger than maximum diameter of the crural bases; descending lamellae very flat but relatively wide; ascending lamellae slender and narrow; transverse band narrow and short and appear at approximately one-third of the length of the dorsal valve. No spine structures on the loop. In serial sections, crural process triangular or parenthesis-shaped, and inclines toward the plane of symmetry; descending lamellae thin arc, and horizontal or very slightly inclined toward the plane of symmetry; ascending lamellae triangular in the

posterior area, becomes thin line anteriorly, and inclines toward the plane of symmetry.

Etymology.—From the Latin, *planus* (*plana*, feminine), denoting the flat shells.

Material.—A total of 32 complete specimens collected from the Early Triassic Kangshare Formation. Of these, three specimens were sectioned (SL-C-SS-001 [Figs. 21, 22], SL-C-SS-002, SL-C-SS-003) and 15 selected specimens were photographed.

Remarks.—Because the overall shape of the loop changes as the shell grows (MacKinnon and Lee, 2006), only by comparing the same growth stage of loops in different species we can accurately identify the differences among several species. Hoover (1979) studied the development of loops in small-sized specimens of *Obnixia thaynesiana* (Girty, 1927) (12.3 mm maximal length, 11.7 mm maximal width). The results indicated that the loop matures (Glossothyropsiform stage; Hoover, 1979, pl. 3, figs. 8–13) when the shell grows to half of its maximum length (3.35–6.6 mm in dorsal length; Hoover, 1979, Table 1). To study the internal structures of *S. plana* n. gen. n. sp., we selected a specimen with a length of 7.25 mm to grind the serial sections because the largest holotype specimen (Fig. 19.71–19.75, SL-C-015, 8.97 mm in length) and the smaller paratype specimens (Fig. 19.66–19.70, SL-C-014, 8.27 mm in length; Fig. 19.61–19.65, SL-C-013, 7.54 mm in length) have only one complete specimen. Therefore, based on ontogeny, this smaller specimen can still typify the adult structure of *S. plana* n. gen. n. sp.

Periallus woodsidensis Hoover, 1979, a narrowly distributed species from western USA (Hoover, 1979; Hofmann et al., 2013), is subtrigonal or oval to subpentagonal in outline, whereas *S. plana* n. gen. n. sp. is subcircular. The anterior commissure of *P. woodsidensis* varies greatly, from rectimarginate to uniplicate or paraplicate, while *S. plana* n. gen. n. sp. shows only a rectimarginate anterior commissure in both adults and juveniles. The mesothyrid foramen of *P. woodsidensis* is larger than that in *S. plana* n. gen. n. sp.. In terms of the internal structures, *P. woodsidensis* has no myophragm in the ventral valve, while *S. plana* n. gen. n. sp. shows a low myophragm in the ventral valve (Figs. 21, 22). The development of inner hinge plates of *P. woodsidensis* is unstable and sometimes completely absent (Fig. 24). Nevertheless, *S. plana* n. gen. n. sp. shows undivided hinge plates (Figs. 21, 24). The septalial plates of *P. woodsidensis* are also variably expressed as short vertical crural plates that connect inner hinge plates to the valve floor or as a low and wide septalium that links the inner hinge plates to the dorsal median septum (Fig. 24). However, *S. plana* n. gen. n. sp. always has a stable septalium (Figs. 21, 24). The crural bases of *P. woodsidensis* arise from the middle of the hinge plates and stretch to the dorsal valve (Fig. 24). Nevertheless, it is quite distinct from *S. plana* n. gen. n. sp. (Figs. 21, 24). There is a substantial difference between *P. woodsidensis* and *S. plana* n. gen. n. sp. in the structure of the loop. *P. woodsidensis* has descending lamellae and broad ascending lamellae that converge anteriorly, but are widely separated. The entire dorsal surface of the descending lamellae is profusely covered with spines (Fig. 24).

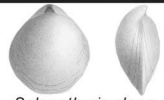
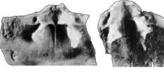
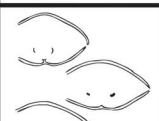
Species	Features	Size	Outline	Profile	Commissure	Myophragm in ventral valve	Cardinal plates	Crural base	Loop		
									Length	Descending and ascending lamellae	Spine
 <i>Selongthyris plana</i> n. gen. n. sp.		small	subcircular, elongated suboval to subpentagonal	ventribiconvex	rectimarginate	have		given off ventrally 	long		without
 <i>Periallus woodsidensis</i> Hoover, 1979		small	subtrigonal, oval to subpentagonal	ventribiconvex	rectimarginate, uniplicate, paralicate	without		given off dorsally 	long		have
 <i>Obnixia thaynesiana</i> (Girty, 1927)		small	subcircular to subpentagonal	ventribiconvex	unisulcate	without		given off ventrally 	long		have
 <i>Protogusarella smithi</i> Perry and Chatterton, 1979		small	elongated suboval to subpentagonal	equally biconvex	rectimarginate, unisulcate	without		given off dorsally 	long		without
 <i>Tosuhuthyris sulcus</i> Sun and Ye, 1982		medium	subpentagonal	ventribiconvex	unisulcate	without		given off ventrally 	short		without

Figure 24. Comparison of the main external and internal features in *Selongthyris plana* Wang and Chen n. gen. n. sp. with *Periallus woodsidensis* Hoover, 1979, *Obnixia thaynesiana* (Girty, 1927), *Protogusarella smithi* Perry and Chatterton, 1979, and *Tosuhuthyris sulcus* Sun and Ye, 1982. The figures of loop are shown by serial sections through posterior to anterior or silicified specimens.

Obnixia thaynesiana has a shallow sulcus anteriorly in the early stages of ontogeny, and forming a unisulcate commissure. However, in all specimens, *S. plana* n. gen. n. sp. has no sulcus, and the anterior commissure still belongs to the rectimarginate type. *O. thaynesiana* has thin and very short deltidial plates, while *S. plana* n. gen. n. sp. shows relatively high and distinct deltidial plates. For the internal structures, *O. thaynesiana* has no myophragm in the ventral valve (Fig. 24), while *S. plana* n. gen. n. sp. has a low myophragm (Figs. 21, 22). *O. thaynesiana* has only a low myophragm and no inner hinge plates, dorsal median septum, or septalium in the dorsal valve (Fig. 24). The descending lamellae and ascending lamellae of *O. thaynesiana* are widely separated and convergent anteriorly. Spines commonly appear at the junction of the descending and ascending lamellae (Fig. 24). All these structures have massive differences compared with *S. plana* n. gen. n. sp. (Figs. 21–24).

Protogusarella smithi Perry and Chatterton, 1979, has a weak sulcus on the dorsal valve and a weak fold on the ventral valve anteriorly, forming a weakly unisulcate to rectimarginate anterior commissure. However, all specimens of *S. plana* n. gen. n. sp. are rectimarginate in the anterior commissure and have no sulcus or fold on the shell surface. The valves of *P. smithi* are equally biconvex in profile, whereas the shells of *S. plana* n. gen. n. sp. are ventribiconvex in profile. The foramen of *P. smithi* belongs to the permesothyrid type, and the deltidial plates are very short and thin. Nevertheless, *S. plana* n. gen. n. sp. has a mesothyrid foramen with high, distinct deltidial plates. As for the internal structures, *S. plana* n. gen. n. sp. has a low myophragm on the ventral valve, while *P. smithi* lacks

myophragm on the ventral valve (Figs. 21, 22, 24). The cardinal plates of the two species have apparent differences (Fig. 24). The inner hinge plates (crural plates) of *P. smithi* are directly connected to the dorsal valve with no median septum or septalium. Besides, the crural bases possibly stretch to the dorsal valve. In addition, in specimens of *P. smithi*, the long and ventrally pointed crural process inclines toward the lateral region, and the descending lamellae and ascending lamellae are widely separated and slightly convergent anteriorly (Fig. 24).

Tosuhuthyris sulcus Sun and Ye, 1982 (holotype specimen: 13.6 mm in length and 13 mm in width; paratype specimen: 13.9 mm in length and 17 mm in width) is larger than *S. plana* n. gen. n. sp. (2.67–8.97 mm in length and 2.57–8.47 mm in width). The dorsal valve of *T. sulcus* has a shallow sulcus that forms a unisulcate anterior commissure. However, *S. plana* n. gen. n. sp. consistently shows a rectimarginate anterior commissure, without any sulcus or fold. In the interior of the ventral valve, *S. plana* n. gen. n. sp. has a low myophragm, but *T. sulcus* does not. The biggest difference between the two species is the loop. The loop of *T. sulcus* is very simple and short, with only descending lamellae and no transverse band, such as a simple crura (Fig. 24). In contrast, *S. plana* n. gen. n. sp. has a long teliform loop (Figs. 21–24).

Reconstruction of ontogeny

In this study, we compared the individual morphological changes of these species in each growth period and found that

the three species showed completely different development patterns. Shell shape of *Piarorhynchella selongensis* Wang and Chen n. sp. changed greatly throughout the growth processes, with very clear differences between juveniles and adults (Figs. 4–9). The juvenile shell has a subtriangular outline with length larger than width (Fig. 8.1) and maximum width located in the middle of the shell. As the shell grows, width grows at a greater rate than length (Fig. 8.1). Its flanks gradually widen, the anterior part of the outline becomes straighter, and the outline gradually becomes subpentagonal. The shell reaches maximum width at three-quarters length towards the anterior. With the growth of the shell, the convexity of the shell also changes (Figs. 4–6, 8.2). Juveniles have flat ventral valves and convex dorsal valves with maximum thickness located at the posterior area. However, adult shells are much more convex with the dorsal valve slightly more convex than that ventral valve, and the maximum thickness in the middle of the shell. Juveniles have smooth shells, very shallow sulcus in the dorsal valve, and less-significant fold in the ventral valve (Fig. 4). As the shell grew, the distribution of the sulcus and fold was reversed: the anterior part of the ventral valve extended forward and bent strongly to form a linguiform extension and the central bulge of the dorsal valve formed a fold (Figs. 4–7). The sulcus and fold gradually developed plicae and form two different development directions (Fig. 7): one in which two plicae appear on the fold and one in which three plicae appear on the fold. Statistics show that there are equal numbers of each type, which shows that these two kinds of shell forms have no special advantages. There are no plicae on the lateral flanks before the shell fold and sulcus become obvious. Where the fold and sulcus emerge, they are flanked by weak plica that appeared on the side of lateral flanks of the two valves, occasionally forming a second shorter and weaker plica on the lateral margin (Figs. 4–6). The anterior commissure becomes increasingly uniplicate through growth, eventually becoming bisulcate in larger shells (Figs. 4–7).

Schwagerispira cheni Wang and Chen n. sp. only showed subtle changes in morphology through development (Figs. 14–16). *S. cheni* n. sp. has the same outline (Figs. 14–16.1), profile (Fig. 16.2), and number of costae (Figs. 14, 15) throughout growth, but the beak becomes slightly curved during shell growth. With the growth of the shell, the narrow median dorsal sulcus, which arises from the umbo area, widened progressively, but remained shallow and becomes indistinct (Figs. 14, 15). As the shell grew, the narrow median costa gradually widened, and finally became wider than other costae in the anterior region (Figs. 14, 15). As the width of the middle costa increased, the top of the middle costa gradually flattened (Figs. 14, 15).

Selongthyris plana Wang and Chen n. gen. n. sp. showed small morphological change through shell growth. The outline (Figs. 19, 20.1) and profile (Fig. 19) of *S. plana* n. gen. n. sp. are roughly the same through development. As the growth rate of the shell decreased, the convexity of the shell gradually increased (Fig. 20.2). However, even in adult specimens, the shells are still very flat (Figs. 19, 20.2). There is no sulcus or fold during growth of the shell, so the anterior commissure of this species is rectimarginate in all specimens (Fig. 19). The beak of the juveniles is slightly incurved and never tangent to the commissure plane. However, as the shell grew, the beak of

the adults became more curved and tangent to the commissure plane.

Brachiopod recovery after the Permian–Triassic extinction

There are nine orders of Permian-type brachiopods (Permian relict brachiopods) in the latest Permian–earliest Triassic strata, including Lingulida, Orthothetida, Orthida, Productida, Spiriferida, Spiriferinida, Rhynchonellida, Athyrida, and Terebratulida (Chen et al., 2005a). All Permian relict brachiopods were extinct before the early Griesbachian, with the exception of some inarticulate brachiopods. Only the Spiriferinida, Rhynchonellida, Athyrida, and Terebratulida survived the extinction (Chen et al., 2005b), sharing several characteristics that clearly differed from the Permian-type brachiopods. In this study, the brachiopods found in the strata of the Early Triassic Kangshare Formation in the Selong section were all typical Mesozoic species. *Piarorhynchella selongensis* Wang and Chen n. sp. belongs to order Rhynchonellida and has very simplified internal and external features. These features consist of a small size, weak and few plicae, a smooth shell surface from the middle to the beak, a ventral valve with thin dental plates with no spondylium or median septum, no complex cardinal process in the dorsal valve, hinge plates, a median septum, a septalium, and raduliform crura in the simplest forms. In comparison to the Permian species of the athyridide *Hustedia*, *Schwagerispira cheni* Wang and Chen n. sp. also belongs to order Athyrida, but it is smaller in size, has less-pronounced and rounded costae, and has simpler cardinal structures. *Selongthyris plana* Wang and Chen n. gen. n. sp., a terebratulide, is characterized by a small size, flat shell, no sulcus or fold, no shell ornaments, and the presence of a simple teloform loop.

The recovery process of brachiopods after the Permian–Triassic mass extinction in southern Tethys remains unclear. The Selong section was a candidate of the Global Stratotype Section and Point of the Permian–Triassic boundary, which spans the late Permian Selong group and the Early Triassic Kangshare Formation. Brachiopod fossils have been studied in detail by Shen et al. (2000, 2001) in the strata of the late Permian Selong Group. Forty-two brachiopod species in 30 genera and two unidentifiable genera that represent a typical big, thick-shelled, Peri-Gondwanan type brachiopod fauna have been recorded. In addition, Shen and Jin (1999) studied brachiopods of the Permian–Triassic boundary beds (*Waagenites* Bed) at Selong. However, the *Waagenites* Bed at the bottom of the Kangshare Formation contained a different group of small- to medium-sized, warm-water brachiopods. This succession process of brachiopods in the Permian–Triassic boundary beds appears in many Peri-Gondwanan regions, such as Salt Range of Pakistan (Grant, 1970), Kashmir (Nakazawa et al., 1975), and north-central Nepal (Waterhouse and Shi, 1990). However, these Permian-type brachiopods did not cross the Permian–Triassic boundary at Selong (Shen and Jin, 1999; Shen et al., 2000; Yuan et al., 2018). In addition, only six Early Triassic brachiopod species have been reported in the Himalayas.

In this study, we found abundant Mesozoic-type brachiopods in Beds 29, 36–42, and 67–70 (late Dienerian–late Smithian, Fig. 2), and their composition and characteristics (as

mentioned above) differ completely from those in the Selong Group and *Waagenites* Bed. *Piarorhynchella selongensis* n. sp. first appeared in Bed 29, corresponding to the late Dienerian. The three new species identified in this study appeared in early Smithian strata (Bed 36). Although there were only three species in this fauna, they were related to three of the four orders of Mesozoic-type brachiopods. Therefore, recovery of brachiopods after the Permian-Triassic mass extinction may have had an initial phase in the early Smithian in the Himalayas.

Late Smithian extinction of brachiopods

Brachiopod diversity decreases gradually up section into the Smithian at Selong. One species, *Schwagerispira cheni* Wang and Chen n. sp., disappeared in the early Smithian, whereas the other two species, *Piarorhynchella selongensis* Wang and Chen n. sp. and *Selongthyris plana* Wang and Chen n. gen. n. sp., disappeared in the late Smithian. These three species did not occur in the overlying black shale interval (Fig. 2) and carbonate rocks that were assigned to the Spathian age.

The disappearance of brachiopods in the late Smithian is consistent with the Smithian-Spathian extinction recognized in the conodont and ammonoid records (Orchard, 2007; Brayard et al., 2009; Stanley, 2009). The late Smithian extinction event may be the result of a series of climatic and environmental events, such as rapid cooling (Sun et al., 2012; Goudemand et al., 2019), significant positive shift in carbon isotopes (Payne et al., 2004; Tong et al., 2007), and widespread anoxia (Song et al., 2012, 2019; Grasby et al., 2013). In this study, we found that brachiopods at Selong suffered extinction during the late Smithian crisis, implying that the diversity loss of brachiopods may have been related to the environmental upheavals in the southern Tethys.

Endemism of Early Triassic brachiopods

Early Triassic brachiopods were widely distributed (Dagys, 1974, 1993; Ager and Sun, 1988; Ke et al., 2016) throughout many areas in the northern hemisphere, from low- to high-latitude areas (South China, western USA, northwest Caucasus, Romania, southern Qilian Mountains of China, Kazakhstan, and South Primorye of Russia), as well as a few areas in the southern hemisphere (Lhasa of China, Spiti of India, and southern Tibet of China). However, the type and composition of brachiopod fauna differed greatly among regions and had distinct local characteristics.

South Primorye of Russia contained an abundance of Early Triassic brachiopods (Griesbachian–Spathian), including all four Early Triassic brachiopods orders. These brachiopods include Rhynchonellida representatives (*Abrekia sulcata* Dagys, 1974; *Paranorellina parisi* Dagys, 1974; and *Piarorhynchella tazawai* Popov in Popov and Zakharov, 2017) (Dagys, 1965, 1974; Shigeta et al., 2009; Zakharov and Popov, 2014; Popov and Zakharov, 2017), a Terebratulida (*Bittnerithyris margaritovi* [Bittner, 1899a,b]) (Bittner, 1899a,b; Dagys, 1965; Popov and Zakharov, 2017), Athyrida representatives (*Spirigerellina pygmaea* Dagys, 1974, and *Hustedtiella planicosta* Dagys, 1972) (Dagys, 1974); and a Spiriferinida (*Lepismatina mansfieldi* [Girty, 1927]) (Dagys, 1965).

There are also many Early Triassic brachiopods (Dienerian–Spathian) in the western USA, mainly consisted of Terebratulida representatives: *Obnixia thaynesiana* (Girty, 1927); *Periallus woodsidensis* Hoover, 1979; *Rhaetina incurvirostra* Hoover, 1979; *Portneufia episulcata* Hoover, 1979; *Vex simplex* Hoover, 1979; and *Protogusarella smithi* Perry and Chatterton, 1979 (Girty, 1927; Hoover, 1979; Perry and Chatterton, 1979; Hofmann et al., 2013, 2014). Only one representative species from each of the orders Rhynchonellida and Spiriferinida (*Piarorhynchella mangyshlakensis* Dagys, 1974 and *L. mansfieldi* [Girty, 1927], respectively) were reported in this region (Girty, 1927; Newell and Kummel, 1942; Perry and Chatterton, 1979; Hofmann et al., 2013). Early Triassic (late Griesbachian, Spathian) brachiopods in South China were characterized by Rhynchonellida and included representatives of *Piarorhynchella gujiaoensis* (Feng and Jiang, 1978), *Laevorhynchia tenuis* Shen and He, 1994, *Meishanorhynchia meishanensis* Chen and Shi in Chen et al., 2002, and *Lichuanorelloides lichuanensis* F.Y. Wang et al., 2017 (Feng and Jiang, 1978; Shen and He, 1994; Chen et al., 2002; F.Y. Wang et al., 2017).

The brachiopod fauna found in the Selong section in this study includes three new and completely different species that belong to three different orders. According to available data, this brachiopod fauna had a very narrow geographical distribution and was only found in southern Tibet, China. Therefore, the brachiopod fauna found in the Selong section had very obvious local characteristics. This made the fauna highly endemic, in contrast to the cosmopolitanism of some groups, such as ammonoids (Dai and Song, 2020).

Conclusions

Here, we report an abundant Early Triassic brachiopod fauna from the Selong section, southern Tibet, China. Among the 825 brachiopod specimens that were collected from the Kangshare Formation were a new terebratulide genus and species (*Selongthyris plana* Wang and Chen n. gen. n. sp.), a new rhynchonellide species (*Piarorhynchella selongensis* Wang and Chen n. sp.), and a new athyridide species (*Schwagerispira cheni* Wang and Chen n. sp.). The ontogenies of these three new species are described in detail, and three completely different ontogenetic patterns are revealed. This brachiopod fauna occurred in the *Neospathodus pakistanensis* and *Neospathodus waageni* conodont biozones and in the *Kashmirites* and *Anasibirites* ammonoid biozones, indicating a late Dienerian–late Smithian age. Recovery of brachiopods after the Permian-Triassic mass extinction in the Himalayas may have reached an initial phase in the early Smithian. The disappearance of this brachiopod fauna at the Smithian-Spathian boundary may be related to the late Smithian extinction event. In addition, the Early Triassic brachiopods are endemic animals with obvious local characteristics.

Acknowledgments

We thank M.-T. Li, and S.-Y. Jiang for their help in the field. We are grateful to C. Sproat, A. Vörös, J.F. Baeza-Carratalá, and J.S. Jin for their affirmation and constructive comments, which

greatly improved the quality of this paper. This study is supported by the National Natural Science Foundation of China (42072010, 41821001, 41672016), Strategic Priority Research Program of Chinese Academy of Sciences (XDB26000000), the Ministry of Education of China, 111 Project (B08030), the National Mineral Rock and Fossil Specimens Resource Center, China. This is also a contribution to International Geosciences Program (IGCP) 630 “Permian and Triassic Integrated Stratigraphy and Climatic, Environmental and Biotic Extremes.”

References

- Ager, D.V., 1959, The classification of the Mesozoic Rhynchonelloidea: *Journal of Paleontology*, v. 33, p. 324–332.
- Ager, D.V., 1965, Mesozoic Rhynchonellacea, in Moore, R.C., ed., *Treatise on Invertebrate Paleontology. Part H, Brachiopoda, Volume 2*. Boulder, Colorado and Lawrence, Kansas, Geological Society of America and University of Kansas Press, p. H597–H625.
- Ager, D.V., 1988, Extinctions and survivals in the Brachiopoda and the dangers of data bases, in Larwood, G.P., ed., *Extinction and Survival in the Fossil Record: Systematics Association Special Publication 34*, p. 89–97.
- Ager, D.V., and Sun, D.L., 1988, Distribution of Mesozoic brachiopods on the northern and southern shores of Tethys: *Palaeontology Cathayana*, v. 4, p. 23–51.
- Ager, D.V., Childs, A., and Pearson, D.A., 1972, The evolution of the Mesozoic Rhynchonellida: *Geobios*, v. 5, p. 157–235.
- Alexander, R.R., 1977, Growth, morphology and ecology of Paleozoic and Mesozoic opportunistic species of brachiopods from Idaho-Utah: *Journal of Paleontology*, v. 51, p. 1133–1149.
- Allan, R.S., 1940, A revision of the classification of the terebratuloid Brachiopoda: *Canterbury Museum, Records*, v. 4, p. 267–275.
- An, X.Y., Zhang, Y.J., Zhu, T.X., Zhang, Y.C., and Yuan, D.X., 2018, Stable carbon isotope characteristics of Permian-Triassic boundary at the Selong Xishan Section: *Earth Science*, v. 43, p. 2848–2857. [in Chinese with English abstract]
- Bitner, A., 1890, Brachiopoden der alpinen Trias: *Abhandlungen der Kaiserlich-Königlichen Geologischen Reichsanstalt*, v. 14, p. 1–325.
- Bitner, A., 1899a, Trias Brachiopoda und Lamellibranchiata: *Memoirs of the Geological Survey of India, Palaeontologia Indica*, ser. 15, v. 3, p. 1–76.
- Bitner, A., 1899b, Versteinerungen aus den Trias-Ablagerungen des Süd-Ussuri Gebietes in der ostsibirischen Küstenprovinz: *Trudy Geologicheskago Komiteta*, v. 7, p. 1–35.
- Boucot, A.J., Johnson, J.G., and Staton, R.D., 1964, On some atrypoid, retzioid, and atrypoid Brachiopoda: *Journal of Paleontology*, v. 38, p. 805–822.
- Brayard, A., Escarguel, G., Bucher, H., Monnet, C., Brühwiler, T., Goudemand, N., Galfetti, T., and Guex, J., 2009, Good genes and good luck: ammonoid diversity and the end-Permian mass extinction: *Science*, v. 325, p. 1118–1121.
- Brühwiler, T., Bucher, H., Brayard, A., and Goudemand, N., 2010, High-resolution biochronology and diversity dynamics of the Early Triassic ammonoid recovery: the Smithian faunas of the Northern Indian Margin: *Palaeogeography, Palaeoclimatology, Palaeoecology*, v. 297, p. 491–501.
- Carlson, S.J., 2016, The evolution of Brachiopoda: *Annual Review of Earth and Planetary Sciences*, v. 44, p. 409–438.
- Chen, J., Ton, J.N., Song, H.J., Luo, M., Huang, Y.F., and Xiang, Y., 2015, Recovery pattern of brachiopods after the Permian-Triassic crisis in South China: *Palaeogeography, Palaeoclimatology, Palaeoecology*, v. 433, p. 91–105.
- Chen, Y.M., 1983, New advance in the study of Triassic brachiopods in Tulong district of Nyalam County, Xizang (Tibet): *Contribution to the Geology of Qinghai-Xizang (Tibet) Plateau*, v. 11, p. 145–156. [in Chinese]
- Chen, Z.Q., Shi, G.R., and Kaiho, K., 2002, A new genus of rhynchonellid brachiopod from the Lower Triassic of South China and implications for timing the recovery of Brachiopoda after the end-Permian mass extinction: *Palaeontology*, v. 45, p. 149–164.
- Chen, Z.Q., Kaiho, K., and George, A.D., 2005a, Survival strategy of brachiopod fauna from the end-Permian mass extinction: *Palaeogeography, Palaeoclimatology, Palaeoecology*, v. 224, p. 232–269.
- Chen, Z.Q., Kaiho, K., and George, A.D., 2005b, Early Triassic recovery of the brachiopod faunas from the end-Permian mass extinction: a global review: *Palaeogeography, Palaeoclimatology, Palaeoecology*, v. 224, p. 270–290.
- Dagys, A.S., 1965, Triasovye Brachiopody Sibiri: *Moscow, Nauka*, 188 p. [in Russian]
- Dagys, A.S., 1972, Morfologiya i systematika Mezozoiskikh retsiodynykh brachiopod: *Akademiya Nauk SSSR, Sibirskoe Otdelenie, Institut Geologii i Geofiziki, Trudy*, v. 112, p. 94–105. [in Russian]
- Dagys, A.S., 1974, Triassic brachiopods (morphology, classification, phylogeny, stratigraphical significance and biogeography): *Akademiya Nauk SSSR, Sibirskoe Otdelenie, Institut Geologii i Geofiziki, Trudy*, v. 214, p. 1–386. [in Russian]
- Dagys, A.S., 1993, Geographic differentiation of Triassic brachiopods: *Palaeogeography, Palaeoclimatology, Palaeoecology*, v. 100, p. 79–87.
- Dai, X., and Song, H.J., 2020, Toward an understanding of cosmopolitanism in deep time: a case study of ammonoids from the middle Permian to the Middle Triassic: *Paleobiology*, v. 46, p. 533–549.
- Dai, X., Song, H.J., Wignall, P.B., Jia, E.H., Bai, R.Y., Wang, F.Y., Chen, J., and Tian, L., 2018, Rapid biotic rebound during the late Griesbachian indicates heterogeneous recovery patterns after the Permian-Triassic mass extinction: *Geological Society of America Bulletin*, v. 130, p. 2015–2030.
- Erwin, D.H., 1994, The Permo-Triassic extinction: *Nature*, v. 367, p. 231–235.
- Feng, R.L., and Jiang, Z.L., 1978, Brachiopoda, in Guizhou Work Team of Stratigraphy and Palaeontology, ed., *Palaeontological Atlas of Southwest China, Guizhou Province, Volume 2*: Beijing, Geological Publishing House, p. 231–304. [in Chinese.]
- Gaetani, M., 1969, Osservazioni paleontologiche e stratigrafiche sull’Anisico delle Giudicarie (Trento): *Rivista Italiana di Paleontologia e Stratigrafia*, v. 75, p. 469–546.
- Gaetani, M., Balini, M., Nicora, A., Giorgioni, M., and Pavia, G., 2018, The Himalayan connection of the Middle Triassic brachiopod fauna from Socotra (Yemen): *Bulletin of Geosciences*, v. 93, p. 247–268.
- Garzanti, E., Nicora, A., and Rettori, R., 1998, Permo-Triassic boundary and Lower to Middle Triassic in South Tibet: *Journal of Asian Earth Sciences*, v. 16, p. 143–157.
- Girty, G.H., 1927, New species of Lower Triassic fossils from the Woodside and Thayne formations, in Mansfield, G.R., ed., *Geography, Geology, and Mineral Resources of Part of Southeastern Idaho, with Descriptions of Carboniferous and Triassic Fossils*: United States Geological Survey Professional Paper, v. 152, p. 434–446.
- Goudemand, N., Romano, C., Leu, M., Bucher, H., Trotter, J.A., and Williams, I.S., 2019, Dynamic interplay between climate and marine biodiversity upheavals during the Early Triassic Smithian-Spathian biotic crisis: *Earth-Science Reviews*, v. 195, p. 169–178.
- Grădinaru, E., and Gaetani, M., 2019, Upper Spathian to Bithynian (Lower to Middle Triassic) brachiopods from North Dobrogea (Romania): *Rivista Italiana di Paleontologia e Stratigrafia*, v. 125, p. 91–123.
- Grant, R.E., 1970, Brachiopods from Permian-Triassic boundary beds and age of Chhidru Formation, West Pakistan, in Kummel, B., and Teichert, C., eds., *Stratigraphic Boundary Problems: Permian and Triassic of West Pakistan*: University of Kansas, Department of Geology, Special Publication 4, p. 117–151.
- Grasby, S., Beauchamp, B., Embry, A., and Sanei, H., 2013, Recurrent Early Triassic ocean anoxia: *Geology*, v. 41, p. 175–178.
- Grunt, T.A., 1986, Sistema brachiopod otriada atiridida: *Akademiya Nauk SSSR, Paleontologicheskii Institut, Trudy*, v. 215, p. 1–200. [in Russian]
- Guo, Z., Chen, Z.Q., and Harper, D.A.T., 2019, The Anisian (Middle Triassic) brachiopod fauna from Qingyan, Guizhou, south-western China: *Journal of Systematic Palaeontology*, v. 18, p. 647–701.
- Hofmann, R., Hautmann, M., Wasmer, M., and Bucher, H., 2013, Palaeoecology of the Spathian Virgin Formation (Utah, USA) and its implications for the Early Triassic recovery: *Acta Palaeontologica Polonica*, v. 58, p. 149–173.
- Hofmann, R., Hautmann, M., Brayard, A., Nützel, A., Bylund, K.G., Jenks, J.F., Vennin, E., Olivier, N., and Bucher, H., 2014, Recovery of benthic marine communities from the end-Permian mass extinction at the low latitudes of eastern Panthalassa: *Palaeontology*, v. 57, p. 547–589.
- Hoover, P.R., 1979, Early Triassic terebratulid brachiopods from the western interior of the United States: *United States Geological Survey Professional Paper*, v. 1057, p. 1–21.
- Jordan, M., 1993, Triassic brachiopods of Romania, in Pálffy, J., and Vörös, A., eds., *Mesozoic Brachiopods of Alpine Europe, Proceedings of the Regional Field Symposium on Mesozoic Brachiopods Vörösbény, Hungary, 6–11 September, 1992*: Budapest, Hungary, Hungarian Geological Society, p. 49–58.
- Jin, Y.G., and Fang, B.X., 1977, Upper Triassic brachiopod fauna from the area in the east of the Hengduan Mountains, western Yunnan, in *Nanjing Institute of Geology and Palaeontology, Chinese Academy of Sciences, ed., Mesozoic Fossils from Yunnan, China, Volume 2*: Beijing, Science Press, p. 39–69. [in Chinese]
- Jin, Y.G., Shen, S.Z., Zhu, Z.L., Mei, S.L., and Wang, W., 1996, The Selong Xishan section, candidate of the global stratotype section and point of the Permian-Triassic boundary, in Yin, H.F., ed., *The Palaeozoic-Mesozoic Boundary Candidates of the Global Stratotype Section and Point of the*

- Permian-Triassic Boundary: Wuhan, China University of Geosciences Press, p. 127–137.
- Ke, Y., Shen, S.Z., Shi, G.R., Fan, J.X., Zhang, H., Qiao, L., and Zeng, Y., 2016, Global brachiopod palaeobiogeographical evolution from Changhsingian (late Permian) to Rhaetian (Late Triassic): Palaeogeography, Palaeoclimatology, Palaeoecology, v. 448, p. 4–25.
- Koken, E., 1900, Über Triassische Versteinerungen aus China: Neues Jahrbuch für Mineralogie Geologie und Paläontologie, v. 1, p. 186–215.
- Kozur, H., and Pjatakova, M., 1976, Die Conodontenart *Anchignathodus parvus* n. sp., eine wichtige Leifform der basalen Trias: Proceedings of the Koninklijke Nederlandse Akademie van Wetenschappen, Series B, v. 79, p. 123–128.
- Kuhn, O., 1949, Lehrbuch der Paläozoologie: Stuttgart, E. Schweizerbart'sche Verlagsbuchhandlung, 326 p.
- Li, M.T., Song, H.J., Algeo, T.J., Wignall, P.B., Dai, X., and Woods, A.D., 2018, A dolomitization event at the oceanic chemocline during the Permian-Triassic transition: *Geology*, v. 46, p. 1043–1046.
- Li, M.T., Song, H.J., Woods, A.D., Dai, X., and Wignall, P., 2019, Facies and evolution of the carbonate factory during the Permian-Triassic crisis in South Tibet, China: *Sedimentology*, v. 66, p. 3008–3028.
- Liao, Z.T., and Sun, D.L., 1974, Triassic brachiopods of southwest China, in Nanjing Institute of Geology and Palaeontology, Chinese Academy of Sciences, ed., *A Handbook of the Stratigraphy and Palaeontology in Southwestern China*: Beijing, Science Press, p. 351–353. [in Chinese]
- MacKinnon, D.I., and Lee, D.E., 2006, Loop morphology and terminology in Terebratulida, in Kaesler, R.L., ed., *Treatise on Invertebrate Paleontology, Part H, Brachiopoda, Revised, Volume 5: Rhynchonelliformea (part)*. Boulder, Colorado and Lawrence, Kansas, Geological Society of America and University of Kansas, p. H1974–H1985.
- Manceñido, M.O., and Motchurova-Dekova, N., 2010, A review of crural types, their relationships to shell microstructure, and significance among post-Palaeozoic Rhynchonellida: *Special Papers in Palaeontology*, v. 84, p. 203–224.
- Manceñido, M.O., and Owen, E.F., 1996, Post-Palaeozoic rhynchonellides: an overview, in Copper, P., and Jin, J.S., eds., *Brachiopods: Proceedings of the Third International Brachiopod Congress*: Rotterdam, A.A. Balkema, p. 368.
- Manceñido, M.O., and Owen, E.F., 2001, Post-Palaeozoic Rhynchonellida (Brachiopoda): classification and evolutionary background, in Brunton, C.H.C., Cocks, L.R.M., and Long, S.L., eds., *Brachiopods Past and Present*: London, The Systematic Association Special Volume Series V, 63, p. 189–200.
- Muir-Wood, H.M., 1955, *A History of the Classification of the Phylum Brachiopoda*: London, British Museum (Natural History), 124 p.
- Nakazawa, K., Kapoor, H.M., Ishii, K., Bando, Y., Okimura, Y., and Tokuoka, T., 1975, The upper Permian and Lower Triassic in Kashmir, India: *Memories of the Faculty of Science, Kyoto University, Geology and Mineralogy*, v. 42, p. 1–106.
- Newell, N.D., and Kummel, B., 1942, Lower Eo-Triassic stratigraphy, western Wyoming and southeast Idaho: *Bulletin of the Geological Society of America*, v. 53, p. 937–996.
- Orchard, M.J., 2007, Conodont diversity and evolution through the latest Permian and Early Triassic upheavals: *Palaeogeography, Palaeoclimatology, Palaeoecology*, v. 252, p. 93–117.
- Orchard, M.J., Nassichuk, W.W., and Rui, L., 1994, Conodonts from the lower Griesbachian *Otoceras latilobatum* bed of Selong, Tibet and the position of the Permian-Triassic boundary: *Canadian Society of Petroleum Geologists*, v. 17, p. 823–843.
- Pálffy, J., 1988, Middle Triassic rhynchonellids from the Balaton Highland (Transdanubian Central Range, Hungary): *Annales Historico-naturales Musei Nationalis Hungarici*, v. 80, p. 25–46.
- Pálffy, J., 2003, The Pelsonian brachiopod fauna of the Balaton Highland: *Geologica Hungarica, Series Palaeontologica*, v. 55, p. 139–158.
- Payne, J.L., Lehmann, D.J., Wei, J., Orchard, M.J., Schrag, D.P., and Knoll, A.H., 2004, Large perturbations of the carbon cycle during recovery from the end-Permian extinction: *Science*, v. 305, p. 506–509.
- Perry, D.G., and Chatterton, B.D.E., 1979, Late Early Triassic brachiopod and conodont fauna, Thaynes Formation, southeastern Idaho: *Journal of Paleontology*, v. 53, p. 307–319.
- Popov, A.M., and Zakharov, Y.D., 2017, Olenekian Brachiopods from the Kamenushka River Basin, South Primorye: new data on the brachiopod recovery after the end-Permian mass extinction: *Paleontological Journal*, v. 51, p. 735–745.
- Sakagami, S., Sciunnach, D., and Garzanti, E., 2006, Late Paleozoic and Triassic bryozoans from the Tethys Himalaya (N India, Nepal and S Tibet): *Facies*, v. 52, p. 279–298.
- Savage, N.M., Manceñido, M.O., and Owen, E.F., 2002, Rhynchonellida. Introduction, in Kaesler, R.L., ed., *Treatise on Invertebrate Paleontology, Part H, Brachiopoda, Revised, Volume 4: Rhynchonelliformea (part)*: Boulder, Colorado and Lawrence, Kansas, Geological Society of America and University of Kansas Press, p. H1027–H1040.
- Shen, S.Z., and He, X.L., 1994, The Changhsingian brachiopods faunas in Guiding, Guizhou: *Acta Palaeontologica Sinica*, v. 33, p. 440–454. [in Chinese with English abstract]
- Shen, S.Z., and Jin, Y.G., 1999, Brachiopods from the Permian-Triassic boundary beds at the Selong Xishan section, Xizang (Tibet), China: *Journal of Asian Earth Sciences*, v. 17, p. 547–559.
- Shen, S.Z., Archbold, N.W., Shi, G.R., and Chen, Z.Q., 2000, Permian brachiopods from the Selong Xishan section, Xizang (Tibet), China, part 1: stratigraphy, Strophomenida, Productida and Rhynchonellida: *Geobios-Lyon*, v. 33, p. 725–752.
- Shen, S.Z., Archbold, N.W., Shi, G.R., and Chen, Z.Q., 2001, Permian Brachiopods from the Selong Xishan section, Xizang (Tibet), China, part 2: palaeobiogeographical and palaeoecological implications. Spiriferida, Athyridida and Terebratulida: *Geobios-Lyon*, v. 34, p. 157–182.
- Shen, S.Z., Zhang, H., Li, W.Z., Mu, L., and Xie, J.F., 2006a, Brachiopod diversity patterns from Carboniferous to Triassic in South China: *Geological Journal*, v. 41, p. 345–361.
- Shen, S.Z., Cao, C.Q., Henderson, C.M., Wang, X.D., Shi, G.R., Wang, W., and Wang, Y., 2006b, End-Permian mass extinction pattern in the northern perigondwanan region: *Palaeoworld*, v. 15, p. 3–30.
- Shi, X.Y., and Grant, R.E., 1993, Jurassic rhynchonellids: internal structures and taxonomic revisions: *Smithsonian Contributions to Paleobiology*, v. 73, p. 1–190.
- Shigetani, Y., Zakharov, Y.D., Maeda, H., and Popov, A.M., 2009, The Lower Triassic System in the Abrek Bay area, South Primorye, Russia: *National Museum of Nature and Science Monographs*, v. 38, p. 1–218.
- Siblík, M., 1994, The brachiopod fauna of the Wetterstein Limestone of the Raxalpe (Austria): *Jahrbuch der Geologischen Bundesanstalt*, v. 137, p. 365–381.
- Siblík, M., and Bryda, G., 2005, Brachiopods from the Upper Triassic reef habitats of the Northern Calcareous Alps (Dachstein Limestone, Hochschwab, Austria): *Rivista Italiana di Paleontologia e Stratigrafia*, v. 111, p. 413–437.
- Song, H.J., Wignall, P.B., Tong, J.N., Bond, D.P.G., Song, H.Y., Lai, X.L., Zhang, K.X., Wang, H.M., and Chen, Y.L., 2012, Geochemical evidence from bio-apatite for multiple oceanic anoxic events during Permian-Triassic transition and the link with end-Permian extinction and recovery: *Earth and Planetary Science Letters*, v. 353–354, p. 12–21.
- Song, H.J., Wignall, P.B., Tong, J.N., and Yin, H.F., 2013, Two pulses of extinction during the Permian-Triassic crisis: *Nature Geoscience*, v. 6, p. 52–56.
- Song, H.Y., Du, Y., Algeo, T.J., Tong, J.N., Owens, J.D., Song, H.J., Tian, L., Qiu, H.O., Zhu, Y.Y., and Lyons, T.W., 2019, Cooling-driven oceanic anoxia across the Smithian/Spathian boundary (mid-Early Triassic): *Earth-Science Reviews*, v. 195, p. 133–146.
- Stanley, S.M., 2009, Evidence from ammonoids and conodonts for multiple Early Triassic mass extinctions: *Proceedings of the National Academy of Sciences of the United States of America*, v. 106, p. 15264–15267.
- Sun, D.L., and Shen, S.Z., 2004, Permian-Triassic brachiopod diversity pattern in South China, in Rong, J.Y., and Fang, Z.J., eds., *Mass Extinction and Recovery-Evidences from the Paleozoic and Triassic of South China*: Hefei, University of Science and Technology of China Press, p. 543–569. [in Chinese]
- Sun, D.L., and Ye, S.L., 1982, Middle Triassic brachiopods from the Tosu Lake area, central Qinghai: *Acta Palaeontologica Sinica*, v. 21, p. 153–173. [in Chinese with English abstract]
- Sun, D.L., Hu, Z.X., and Chen, T.E., 1981, Discovery of the upper Permian strata in Lasa, Xizang: *Journal of Stratigraphy*, v. 5, p. 139–142. [in Chinese with English abstract]
- Sun, D.L., Xu, G.R., and Qiao, L., 2017, Triassic brachiopod genera on type species of China, in Rong, J.Y., Jin, Y.G., Shen, S.Z., and Zhan, R.B., eds., *Phanerozoic Brachiopod Genera of China*: Beijing, Science Press, p. 883–1011.
- Sun, Y.D., Joachimski, M.M., Wignall, P.B., Yan, C.B., Chen, Y.L., Jiang, H.S., Wang, L.N., and Lai, X.L., 2012, Lethally hot temperatures during the Early Triassic greenhouse: *Science*, v. 338, p. 366–370.
- Sweet, W.C., 1970, Uppermost Permian and Lower Triassic conodonts of the Salt Range and Trans-Indus ranges, West Pakistan, in Kummel, B., and Teichert, C., eds., *Stratigraphic Boundary Problems: Permian and Triassic of West Pakistan*: University of Kansas Department of Geology Special Publication 4, p. 207–275.
- Tong, J.N., Zuo, J.X., and Chen, Z.Q., 2007, Early Triassic carbon isotope excursions from South China: proxies for devastation and restoration of marine ecosystems following the end-Permian mass extinction: *Geological Journal*, v. 42, p. 371–389.
- Urošević, D., Radulović, V., and Pešić, L., 1992, Middle Triassic (Anisian) brachiopods from the Yugoslavian Carpatho-Balkanides: *Revue de Paleobiologie*, v. 11, p. 469–481.

- Waagen, W.H., 1883, Salt Range fossils. I. *Productus*-Limestone fossils: Memoirs of the Geological Survey of India, Palaeontologia Indica (ser. 13), v. 4, p. 391–546.
- Waagen, W.H., 1895, Salt Range Fossils. Fossils from the Ceratite Formation: Memoirs of the Geological Survey of India, Palaeontologia Indica (ser. 13), v. 4, p. 1–323.
- Wang, F.Y., Chen, J., Dai, X., and Song, H.J., 2017, A new Dienerian (Early Triassic) brachiopod fauna from South China and implications for biotic recovery after the Permian-Triassic extinction: Papers in Palaeontology, v. 3, p. 425–439.
- Wang, L.N., Wignall, P.B., Sun, Y.D., Yan, C.B., Zhang, Z.T., and Lai, X.L., 2017, New Permian-Triassic conodont data from Selong (Tibet) and the youngest occurrence of *Vjalovognathus*: Journal of Asian Earth Sciences, v. 146, p. 152–167.
- Wang, Y.G., and He, G.X., 1976, Triassic Ammonoids from the Mount Jolmo Lungma region, in Xizang Scientific Expedition Team of Chinese Academy of Science, ed., A Scientific Expedition in the Mount Jolmo Lungma Region (1966–1968). Palaeontology: Beijing, Science Press, fasc. 3, p. 223–502. [in Chinese]
- Wang, Y.G., Chen, C.Z., Rui, L., Wang, Z.H., Liao, Z.T., and He, J.W., 1989, A potential global stratotype of Permian-Triassic boundary, preliminary report on Selong-Xishan section, southern Tibet, in Sun, S., Li, Z.Q., Zhao, S.C., Xu, Z.L., Li, P.Y., and Jiang, F.E., eds., Developments in Geoscience: Contributions to the 28th International Geological Congress: Beijing, Science Press, p. 221–230.
- Wang, Z.H., and Wang, Y.G., 1995, Permian–Lower Triassic conodonts from Selong Xishan of Nyalam, South Tibet, China: Acta Micropalaeontologica Sinica, v. 12, p. 333–348. [in Chinese with English abstract]
- Waterhouse, J.B., and Shi G.R., 1990, Late Permian brachiopod faunules from the Marsyangdi Formation, north central Nepal, and the implications for the Permian-Triassic boundary, in Mackinnon D.I., Lee D.E., and Campbell J.D., eds., Brachiopods Through Time: Rotterdam, Balkema, p. 381–387.
- Williams, A., Brunton, C.H.C., Carlson, S.J., Alvarez, F., Blodgett, R.B. et al. 2002, Rhynchonellida (part), in Kaesler R.L., ed., Treatise on Invertebrate Paleontology, Part H, Brachiopoda, Revised, Volume 4: Rhynchonelliformea (part): Boulder, Colorado and Lawrence, Kansas, Geological Society of America and University of Kansas, p. H1027–H1376, H1496–H1613.
- Williams, A., Brunton, C.H.C., Carlson, S.J., Baker, P.G., Carter, J.L. et al. 2006, Rhynchonelliformea (part), in Kaesler, R.L., ed., Treatise on Invertebrate Paleontology, Part H, Brachiopoda, Revised, Volume 5: Rhynchonelliformea (part). Boulder, Colorado and Lawrence, Kansas, Geological Society of America and The University of Kansas, p. H1877–H1937, H1965–H2250.
- Xu, G.R., and Grant, R.E., 1994, Brachiopods near the Permian-Triassic boundary in South China: Smithsonian Contributions to Paleobiology, v. 76, p. 1–68.
- Xu, G.R., and Liu, G.C., 1983, Analyses of the faunas. Systematic description. 1. Some problems in the research of Triassic brachiopods. 2. Brachiopods, in Yang, Z.Y., Xu, G.R., Wu, S.B., He, Y.L., Liu, G.C., and Yin, J.R., eds., Triassic of the South Qilian Mountains: Beijing, Geological Publishing House, p. 34–36, 67–83, 84–123. [in Chinese with English abstract]
- Yang, Z.Y., and Xu, G.R., 1966, Triassic Brachiopods of Central Guizhou Province, China: Beijing, Geological Publishing House, 122 p. [in Chinese]
- Yao, J.X., and Li, Z.S., 1987, Permian–Triassic conodont faunas and the Permian-Triassic boundary at the Selong Section in Nyalam County, Xizang, China: Chinese Science Bulletin, v. 32, p. 1555–1560. [in Chinese with English abstract]
- Yuan, D.X., Zhang, Y.C., and Shen, S.Z., 2018, Conodont succession and reassessment of major events around the Permian-Triassic boundary at the Selong Xishan section, southern Tibet, China: Global Planetary Change, v. 161, p. 194–210.
- Zakharov, Y.D., and Popov, A.M., 2014, Recovery of brachiopod and ammonoid faunas following the end-Permian crisis: additional evidence from the Lower Triassic of the Russian Far East and Kazakhstan: Journal of Earth Science, v. 25, p. 1–44.

Accepted: 27 November 2021